

Lie similarity transformations and Lie control parameters for heat transfer on unsteady stretching surface along with variable heat source or sink



By

Muhammad Saad Anwar
(Registration No: 00000327878)

Department of Mechanical Engineering
School of Mechanical and Manufacturing Engineering
National University of Sciences & Technology (NUST)

Islamabad, Pakistan

(2024)

Lie similarity transformations and Lie control parameters for heat transfer on unsteady stretching surface along with variable heat source or sink



By

Muhammad Saad Anwar

(Registration No: 00000327878)

A thesis submitted to the National University of Sciences and Technology, Islamabad,

in partial fulfillment of the requirements for the degree of

Master of Science in
Mechanical Engineering

Supervisor: Dr. Muhammad Safdar

School of Mechanical and Manufacturing Engineering

National University of Sciences & Technology (NUST)

Islamabad, Pakistan

(2024)

THESIS ACCEPTANCE CERTIFICATE

Certified that final copy of MS/MPhil thesis written by **Regn No. 00000327878 Muhammad saad Anwar** of **School of Mechanical & Manufacturing Engineering (SMME)** has been vetted by undersigned, found complete in all respects as per NUST Statues/Regulations, is free of plagiarism, errors, and mistakes and is accepted as partial fulfillment for award of MS/MPhil degree. It is further certified that necessary amendments as pointed out by GEC members of the scholar have also been incorporated in the said thesis titled. **Lie similarity transformations and Lie control parameters for heat transfer on unsteady stretching surface along with variable heat source or sink.**

Signature: _____

Name of Supervisor Dr. Muhammad Safdar

Date: 08 - Oct - 2024

Signature (HOD): _____

Date: 08 - Oct - 2024

Signature (Dean/ Principal) _____

Date: 08 - Oct - 2024

CERTIFICATE OF APPROVAL

This is to certify that the research work presented in this thesis, entitled “Lie similarity transformations and Lie control parameters for heat transfer on unsteady stretching surface along with variable heat source or sink” was conducted by Mr. Muhammad Saad Anwar under the supervision of Dr. Muhammad Safdar.

No part of this thesis has been submitted anywhere else for any other degree. This thesis is submitted to the SMME NUST in partial fulfillment of the requirements for the degree of Master of Science in Field of Mechanical Engineering.

Department of Mechanical Engineering, SMME, National University of Sciences and Technology, Islamabad.

Student Name: Muhammad Saad Anwar

Signature: _____



Examination Committee:

a) External Examiner 1: Name: Dr. Riaz Ahmad Khan

Designation: Assistant Professor

b) External Examiner 2: Name: Dr. Tauqeer Nasir

Designation: Assistant Professor

c) External Examiner 3: Name: Dr. Saad Ayub Jajja

Designation: Assistant Professor

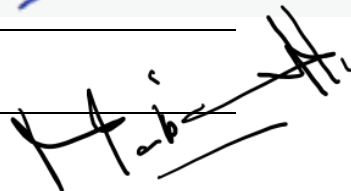
Supervisor Name: Dr. Muhammad Safdar

Signature: _____



Name of HOD: Dr. Mian Ashfaq

Signature: _____



AUTHOR'S DECLARATION

I Muhammad Saad Anwar hereby state that my MS thesis titled “Lie similarity transformations and Lie control parameters for heat transfer on unsteady stretching surface along with variable heat source or sink” is my own work and has not been submitted previously by me for taking any degree from National University of Sciences and Technology, Islamabad or anywhere else in the country/ world.

At any time if my statement is found to be incorrect even after I graduate, the university has the right to withdraw my MS degree.

Name of Student: Muhammad Saad Anwar

Date: 08/10/2024

PLAGIARISM UNDERTAKING

I solemnly declare that research work presented in the thesis titled “Lie similarity transformations and Lie control parameters for heat transfer on unsteady stretching surface along with variable heat source or sink” is solely my research work with no significant contribution from any other person. Small contribution/ help wherever taken has been duly acknowledged and that complete thesis has been written by me.

I understand the zero tolerance policy of the HEC and National University of Sciences and Technology (NUST), Islamabad towards plagiarism. Therefore, I as an author of the above titled thesis declare that no portion of my thesis has been plagiarized and any material used as reference is properly referred/cited.

I undertake that if I am found guilty of any formal plagiarism in the above titled thesis even after award of MS degree, the University reserves the rights to withdraw/revoke my MS degree and that HEC and NUST, Islamabad has the right to publish my name on the HEC/University website on which names of students are placed who submitted plagiarized thesis.

Student Signature: _____



Name: Muhammad Saad Anwar

Dedicated To My Parents

Acknowledgements

I would like to begin by acknowledging the grace and mercy of ALLAH, without whom none of this would have been possible. I am grateful for His guidance, blessings, and protection throughout this academic journey.

I would also like to express my deepest gratitude to my parents for their unwavering support. Their love, encouragement, and sacrifices have been my guiding light and motivation. I am immensely blessed to have them as my parents.

I am deeply indebted to my advisor, Muhammad Safdar, for his invaluable guidance, encouragement, and feedback. His expertise, patience, and commitment to excellence have been instrumental in shaping this thesis. His insightful feedback, constructive criticism, and expert guidance have helped me grow both as a researcher and as a person.

I am fortunate to have such an amazing mentor who has not only supported me throughout the research process but also challenged me to push the boundaries of my knowledge and skills. His mentorship has been transformative and has inspired me to pursue excellence in all aspects of my life.

I am extremely thankful to the members of Guidance and Examination Committee (GEC), Dr. Riaz Ahmad Khan, Dr. Tauqeer Nasir, and Dr. Saad Ayub their invaluable contributions in the form of instructive guidance, beneficial suggestions, and enlightening remarks. Lastly, I would like to extend my heartfelt appreciation to all my friends and colleagues for their support, motivation, and inspiration. Your presence in my life has been a tremendous blessing.

Thank you all, and may God bless you abundantly.

Muhammad Saad Anwar

Table of Contents

Table of Contents.....	9
Abstract.....	11
Chapter 1: Introduction	12
1.1 Lie similarity transformation.....	12
1.2 Background	13
1.3 Motivation.....	14
1.4 Solution procedure:	18
Chapter 2: Literature review.....	19
2.1 Unsteady film flow over stretching surface:	19
2.2 Effect of fluid properties and thermocapillarity:	22
2.3 Effect of viscous dissipation on surface temperature:	22
2.4 Effect of magnetic field and thermocapillarity on unsteady film flow	22
2.5 Effect of internal heating on an unsteady film flow	23
2.6 Other researches:	23
Chapter 3: Methodology.....	25
3.1 Lie symmetry.....	25
3.2 Governing equations.....	25
3.3 Generation of symmetries	26
3.4 Construction of invariants:	27
3.5 Construction of reduced differential equation:	28
3.6 Second reduction.....	28
3.7 Homotopy perturbation method (HPM).....	30
Chapter 4: Results.....	33
4.1 Influence of unsteadiness parameter ‘S’.....	33
4.2 Influence of Prandtl number ‘Pr’.....	35
4.3 Influence of control parameters.....	40
4.3.1 Influence of P4, P5 and P10	40
4.3.2 Influence of P9.....	40
4.3.3 Influence of P7.....	45
4.3.4 Influence of P8.....	47

Chapter 5: Conclusion	50
References	52
Appendix	55

Abstract

The idea of this research is to analyze the flow on time dependent extending surface with changing heat flux. With the variable heat flux, we impose unsteadiness in the flow and temperature fields. We have developed a reduction procedure which provides a few parameters in reduced formats of differential equations which control flow and heat transfer rate. This idea uses the approach of Lie point symmetry to reduce a non-linear model of partial differential equations representing the flow to simplest form of the model in terms of ordinary differential equations. The reduced flow model consists of a set of control parameters. This non-linear model of differential equations is then solved by using Homotopy perturbation method (HPM). Codes are developed on MAPLE which has built in packages for many mathematical applications. These codes are tested and validated in a rigorous manner. As a result, we obtain a set of multiple solutions for velocity and temperature profiles by varying the control parameters. The effect of certain key parameters on velocity profile and temperature distribution are investigated with the help of graphs and Tables using the codes already available and refining them according to the requirement of flow model. Numerical results are compared with published data in certain cases, and reasonably good agreement is established between them. The effects of the Prandtl number and the unsteadiness parameter on flow and heat transfer have also been analyzed.

Chapter 1: Introduction

The heat transfer process taking place through an extending surface is an important topic within the domains of fluid dynamics as well as heat transfer. This phenomenon is of great relevance to a wide variety of practical applications across many disciplines of engineering as well as in various industrial processes like materials processing, chemical engineering, and aerospace engineering. As of late, the traditional issue of the heat transfer over a stretching surface has been stretched out to incorporate non-uniform limit conditions and unsteady condition [1-3] which model a precisely genuine situation. The introduction of an unsteady extending surface and variable heat flux adds intricacy to the issue, making it really testing and challenging.

Studies have been carried out to analyze the effect of thermocapillarity, internal heat source or sink, and a variable magnetic field over an extending surface using Lie symmetry analysis [4]. Similarly, analytical solutions of unsteady thin film flow with internal heating and thermal radiation have also been studied by many researchers [5]. In this research, the complex problem of flow and heat transfer on an unsteady stretching surface with variable flux has been analyzed using Lie point symmetry analysis.

The objective of this research is as follows:

- To investigate the application of Lie similarity transformation and Lie control parameters for the variable heat transfer process taking place through an extending surface.
- Developing of a reduction procedure that provides several parameters in reduced formats of differential equations which actually controls the flow and heat transfer rate.
- A model consisting of several control parameters is obtained. Thus, multiple solutions are obtained by varying the control parameters one by one.

1.1 Lie similarity transformation

The heat transfer over an unsteady stretching surface with variable heat source or sink is a complex problem. In order to solve this kind of problem, some powerful technique must be employed. Lie similarity transformation is a robust procedure for solving such kind of complex problems. It is basically a procedure to transform partial differential equations into a system of ordinary differential equations. It employs the concept of Lie symmetry generation and construction of invariants. As a result, a system of non-linear ordinary differential equations (ODEs) is obtained. Thus helping in understanding the behavior of flow over an unsteady extending surface with variable heat source or sink.

Lie control parameters are important parameters in the employment of Lie similarity transformation which control the flow behavior. In this technique, several Lie control parameters are obtained while solving a complex problem, so multiple solutions are

obtained through this method. This in turn provides the most efficient and optimized solution of the problem.

1.2 Background

The investigation of flow over an unsteady surface was first presented by Sakiadis [6] in 1961, who carried out analysis on the boundary layer flow over a continuous flat sheet moving with a constant velocity. From that point forward, various examinations have stretched out this work to different perspectives, including heat transfer, mass transfer, and non-Newtonian liquids. Nonetheless, most of these examinations studied state of steady flow and constant heat transfer, which isn't generally the situation in practical applications.

A boundary layer is a thin layer of liquid and gas that streams along a surface. The fluid experiences shear forces and shows variable velocities in the boundary layer, changing from zero velocity at the surface to a maximum velocity matching the free stream value at a maximum distance from the surface.

The molecules which are closer to the surface slow down the molecules above them as the fluid passes an object. This in turn slows down the flow above them that is a region of changing velocity. A no slip boundary condition, which means velocity is zero at the surface, is created by the interaction of fluid with the surface.

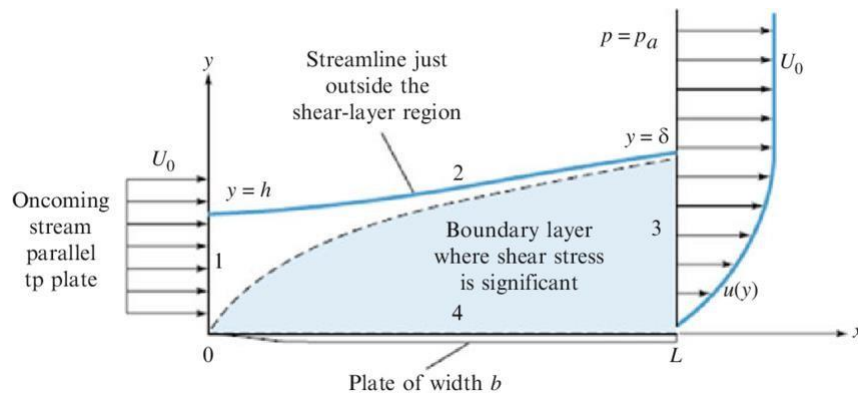


Figure 1.1: Hydrodynamic Boundary layer [7]

In Figure 1.1, fluid is flowing along the surface of flat plate with the velocity of U_0 . Interaction of a fluid with the flat plate creates a no-slip boundary condition where it yields a velocity equal to zero on the wall. Viscous forces acting between adjacent fluid layers are responsible for deceleration of the flow thereby enabling the development of a boundary layer. The velocity of the fluid therefore changes from zero on the wall to the free stream velocity U_0 when moved away from the wall.

Both velocity and thermal boundary layers form due to the temperature differential between the fluid and the surface of some object, and most heat transfer occurs within the region of the velocity boundary layer. There are many practical examples

of the boundary layer condition. It occurs by a flow within a pipe or around the wing of an airplane. The flow changes from laminar to turbulent within a boundary layer.

1.3 Motivation

There are a number of practical applications for a flow over an unsteady extending surface with a variable heat source or sink. One of the applications is to carry out the analysis of the aerodynamic forces on aircraft and wind turbines. Whenever the fluid flows over an aerodynamic shape like an airfoil, generation of boundary layer occurs around that object. Flow passes faster on one side than the other, which generates the lift force. This force is responsible for the flying of an airplane,

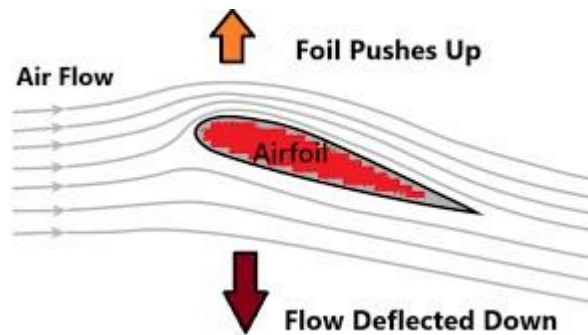


Figure 1.2: Flow around an airfoil ¹

The research of flow over an unsteady stretching surface finds its application in the rotation of wind and water turbines. Lift force increases with the increase in angle of attack of an airfoil, but it can also be increased by improving the shape of an object and it is only possible by analyzing its boundary layer.



Figure 1.3: Wind Turbine²

¹ https://cfdfloengineering.com/basic-of-airfoils-aerodynamics-its-application-and-cfd-modeling/#google_vignette

² <https://www.amazon.sa/-/en/YQWHL-Permanent-Generator-Streetlight-Controller/dp/B09D89T16N>

It is also useful in polymer processing technique. Some of the common polymer processing techniques include extrusion, injection molding, blow molding, thermoforming, etc.

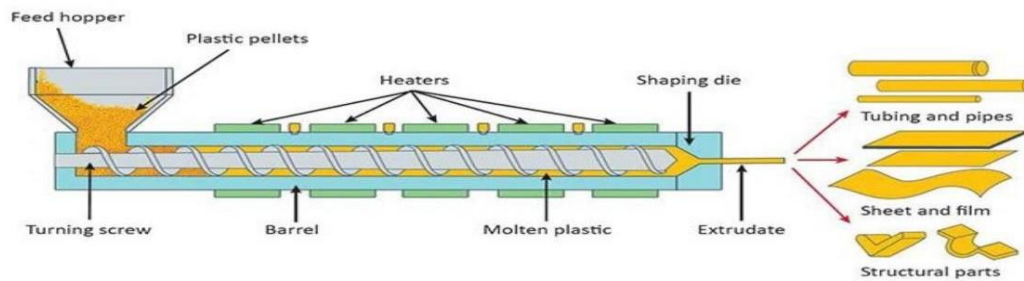


Figure 1.4: Polymer Processing³

The research also finds its application in biomedical engineering [8] as behavior of the flow of blood in arteries is very similar, which helps in understanding cardiovascular diseases.

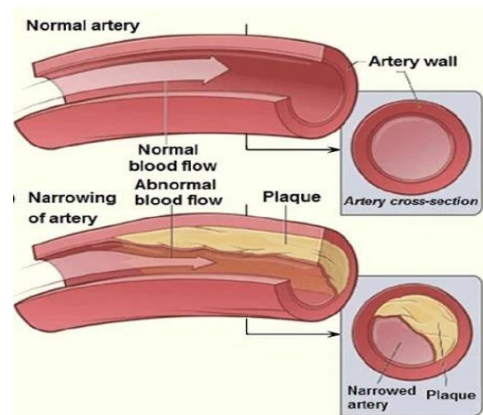


Figure 1.5: Flow of blood in arteries⁴

The study is also useful in the design of aircraft. This study of flow and heat transfer is also important in chemical processing and Material processing techniques such as metal forming and glass manufacturing [9] as well. By directing the temperature distribution and controlling the movement of materials, the study of flow and heat transfer affects the quality, consistency, and efficiency of the final product along with ensuring proper solidification or deformation during the manufacturing process; essentially, understanding how heat and fluid flow interact allows for optimization of process parameters to achieve desired outcomes.

³ <https://jiejatwinscrew.com/blog/the-ultimate-guide-to-plastic-extruder-machines/>

⁴ <https://discover.hubpages.com/health/Signs-and-Symptoms-of-Clogged-Arteries>

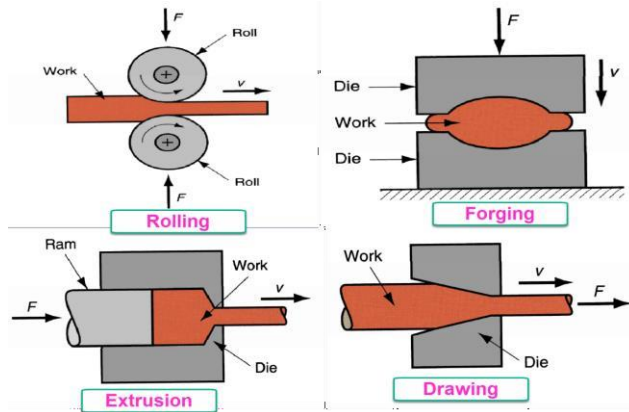


Figure 1.6: Metal Forming⁵

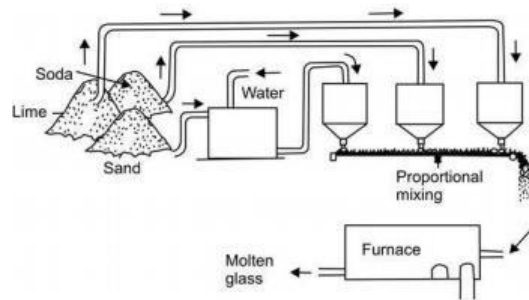


Figure 1.7: Glass Manufacturing⁶

In order to solve environmental pollution and other issues, the study of flow and heat transfer process taking place through an extending surface can play an important role. The study of flow and heat transfer is also relevant in understanding ocean currents [10].

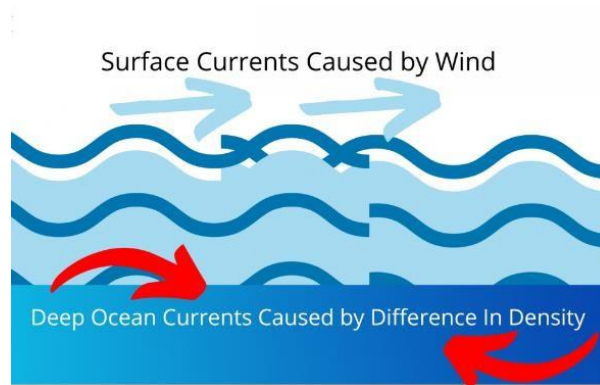


Figure 1.8: Ocean Currents⁷

⁵ https://learnmech.com/metal-forming-basic-types-diagram-classification/#google_vignette

⁶ https://www.brainkart.com/article/Glass_3659/

⁷ <https://spectacularsci.com/2022/08/what-are-ocean-currents/>

The research has an important application in the manufacturing of solar panels. The manufacturing process is unsteady and demands precise control over temperature. The process of controlling the heat generation and the cooling mechanisms by stretching surfaces assures the presence of an electronic property without having the thermal damage along with durability. The current research finds the great application in manufacturing and working mechanism of solar panels.

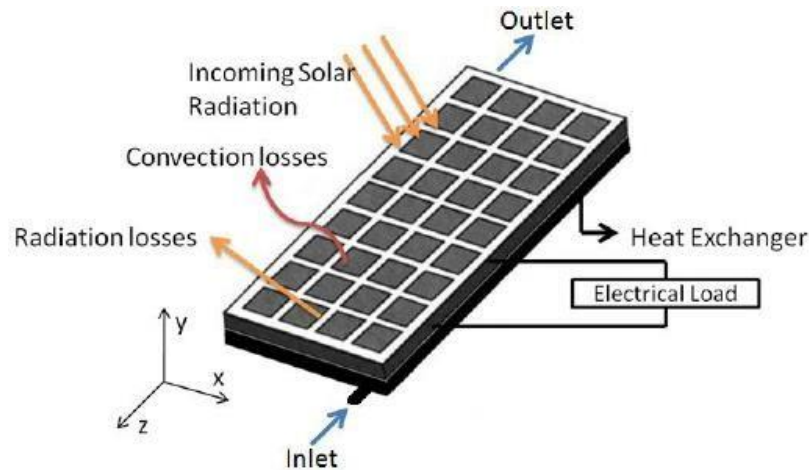


Figure 1.9: Solar Panels⁸

Heat transfer study over an unsteady surface is beneficial in the textile fiber production processes as well. During the synthesis of synthetic fibers, such as nylon and polyester, fibers are pulled over a rough stretchy surface. This requires temperature control to attain desired tensile strength.



Figure 1.10: Textile Fiber Production⁹

⁸ https://www.researchgate.net/figure/MODES-OF-ENERGY-TRANSFER-IN-A-PV-PANEL_fig1_259391190

⁹ https://en.wikipedia.org/wiki/Textile_manufacturing#/media/File:Catalonia_Terrassa_mNATEC_CardaObridora.jpg

Furthermore, the research is extremely beneficial in the study of the formation of thin films in microelectronics. All of these applications show the importance of flow and heat transfer, as they can pave the way for efficient designs, optimized processes, with better and improved performance in various engineering and industrial fields.

1.4 Solution procedure:

Accurately predicting the heat transfer behavior in such systems is a challenging task, and finding optimal solutions for various design and operational parameters is necessary. To address this challenge, this thesis aims to analyze the heat transfer behavior in a liquid film that is stretched in an unsteady manner using Lie point similarity technique. Lie point symmetry is employed to reduce a non-linear model of differential equations representing the flow to simplest form of the model in terms of ordinary differential equations. The reduced flow model consists of a set of control parameters. The research utilized a very efficient analytical technique, known as HPM, to investigate the problem. To ensure the credibility and precision of the results, they were verified and compared against existing literature.

Chapter 2: Literature review

Flow over an unsteady surface has a number of practical applications and a lot of studies on it have been done. Heat transfer across such types of surfaces has also been studied in detail. Such flows are characterized by their dynamics and time-varying nature, and they occur in a wide range of physical and engineering systems, such as coating and drying processes [11], lubrication of mechanical components, and the formation of thin films in microelectronics. The extending motion generates hydrodynamic and thermal boundary layers.

Understanding the intricate dynamics that govern the behavior of boundary layers is crucial for significantly improving the manufacturing process. This understanding is essential not only for optimizing the efficiency of production methods but also for guaranteeing the high quality of the final product that reaches consumers. In all of these applications, the flow behavior is affected by a wide range of factors, like the material properties, the extending rate, and the fluid properties. The noisy boundary conditions, particularly that of an extending sheet, make it difficult to apply both experimental and numerical methods. In this context, similarity solutions emerge as invaluable resources that researchers use to obtain solutions of interest for the flow generated by the extending surface. These flows are effectively addressed through the application of a strategic combination of both theoretical and experimental approaches, in addition to computational techniques. These computational methods include, but are not limited to, the RKF shooting method, the Homotopy analysis method, the finite difference method, and the Homotopy perturbation method, among others. The utilization of these diverse methods is instrumental in gaining a comprehensive understanding of the properties associated with the flow in question.

2.1 Unsteady film flow over stretching surface:

Wang studied the thin film of Newtonian fluid on an unsteady stretching surface and investigated the hydrodynamic behavior of this kind of flow numerically [12]. A film of fluid on a surface which moves along the x-axis of cartesian coordinate system with velocity that changes with time is considered by Wang [12]. The schematic diagram of flow is shown in Figure 2.1. $U(t, x)$ is time-dependent extending velocity of surface and velocity of fluid along x and y axis are u and v respectively. $h(t)$ is boundary layer thickness and it is a function of time.

Wang considered the Navier-Stokes equations of the flow and adopted the similarity transformation procedure to transform the partial differential equations (PDEs) into ODEs. Then he solved the obtained ODEs numerically. Wang's solution did not give any idea of the heat transfer in a liquid film as Wang only considered the conservation of momentum.

Wang [12] considered an unsteady 2D flow on a horizontal elastic sheet of uniform thickness $h(t)$, which propagates through a narrow slit as shown in Fig 2.1.

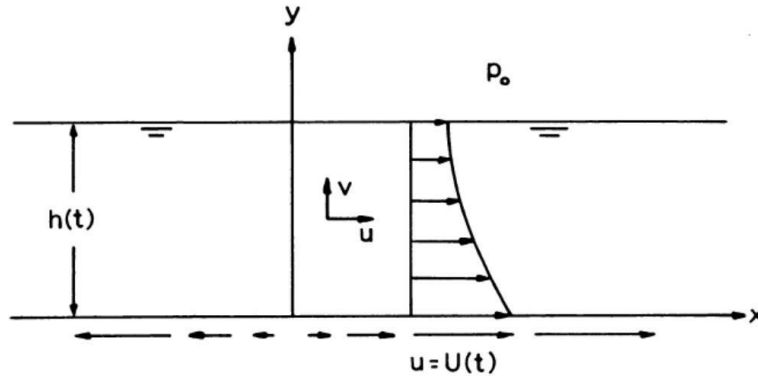


Figure 2.1: Film flow on an unsteady extending surface

The velocity and temperature of Wang [12] model is given by following boundary layer equations:

$$\begin{aligned} \frac{\partial u}{\partial x} + \frac{\partial v}{\partial y} &= 0, \\ \frac{\partial u}{\partial t} + u \frac{\partial u}{\partial x} + v \frac{\partial u}{\partial y} &= \frac{\mu}{\rho} \frac{\partial^2 u}{\partial y^2} \\ \frac{\partial T}{\partial t} + u \frac{\partial T}{\partial x} + v \frac{\partial T}{\partial y} &= \kappa \frac{\partial^2 T}{\partial y^2}. \end{aligned} \quad (2.1)$$

In system of equations 2.1, u and v are velocities along the x and y axis respectively whereas T refers to inside temperature, μ is viscosity, κ is the thermal conductivity and ρ is the fluid density. The above model consists of three dependent variables u , v and T subjected to three independent variables x , y and t .

Wang also considered the following boundary conditions subjected to the system 2.1:

$$\begin{aligned} y = 0, \quad u(x, t) &= U(x, t), \quad v(x, t) = 0, \quad T(x, t) = T_s, \\ y = h(t), \quad \frac{\partial u}{\partial y}(x, t) &= \frac{\partial T}{\partial y}(x, t) = 0, \quad v(x, t) = \frac{dh}{dt}, \end{aligned} \quad (2.2)$$

where U is used to represent velocity at the surface, and q represents the temperature of the extending sheet. Furthermore, $h(t)$ represents the thickness of the film, which is a quantity describing the free surface height of the film. It is assumed that $h(t)$ depends only on time and is constant. $\frac{\partial u}{\partial y} = 0$, implies that the influence of surface tension is ignored and fluid flows only because of the viscous shear developed due to extending of the sheet. $\frac{\partial T}{\partial y} = 0$, implies that the free surface of the liquid film is thermally insulated while the last boundary condition is a kinematic constraint allowing free surface movement.

In order to reduce the non-linear model of PDEs given in system of equations 2.1 to a system of non-linear ODEs, Wang et al. used the following relations:

$$\eta = \sqrt{\frac{b}{v(1-\alpha t)}} y, \quad (2.3)$$

$$u = \frac{bx}{(1-\alpha t)} f'(\eta), \quad (2.4)$$

$$v = -\beta \sqrt{\frac{vb}{(1-\alpha t)}} f(\eta), \quad (2.5)$$

$$T = T_0 - T_{ref} \frac{bx^2}{2v(1-\alpha t)^2} \theta(\eta). \quad (2.6)$$

The extending surface velocity and temperature as

$$U = \frac{bx}{(1-\alpha t)}, \quad (2.7)$$

$$T_S = T_0 - T_{ref} \frac{bx^2}{2v(1-\alpha t)^2}. \quad (2.8)$$

T_0 refers to the slit temperature and T_{ref} refers to the reference temperature for all $t < 1/\alpha$. The specific forms of velocity and temperature are chosen so that transformation 3.3 – 3.6 map the governing system of equations 3.1 – 3.2 to

$$f''' + \beta^2 (ff'' - f'^2 - Sf' - \frac{\xi}{2}\eta f'') = 0, \quad (2.9)$$

$$\frac{\theta^{FF}}{Pr} + \beta^2 (f\theta' - 2f'\theta - \frac{\xi}{2}\eta\theta' - \frac{\xi}{2}S\theta) = 0. \quad (2.10)$$

Subjected to:

$$f'(0) = 1, f(0) = 0, \theta(0) = 1, f''(1) = \theta'(1) = 0, f(1) = \frac{S}{2}. \quad (2.11)$$

Here differentiation is w.r.t η , while $\gamma = \beta^2$ is the dimensionless film thickness, $S = \alpha/b$ is the measure of unsteadiness and $Pr = \nu/\kappa$ is the Prandtl number.

Anderson [13] considered the conservation of mass, momentum and heat energy equations for the same flow while considering a thin elastic sheet of fluid that emerges from a narrow slit at the origin of Cartesian coordinate system. Anderson revealed in his research that the same exact similarity which Wang used in his research can also be obtained for the temperature field. He employed multiple shooting subroutine (MUSN)

method to solve the system of ODEs. He carried out this research for better understanding the heat transfer characteristics of fluid flow which was solved by Wang. And as a result, he succeeded in providing an accurate solution of heat flow problem covering a range of Prandtl number.

Wang [14] solved the system of ODEs for the thin film flow over an extending surface using Homotopy analysis method whereas Anderson used multiple shooting subroutine (MUSN) method. Later Anderson solved the same problem for the other special cases using fifth order Runge-Kutta method [15].

2.2 Effect of fluid properties and thermocapillarity:

B. S. Dandapat [16] has analytically studied the flow behavior of elastic sheet of a flow emerging from a small opening located at the origin of Cartesian coordinate. The movement within the fluid is caused by the extension of the sheet, at which the thin film of fluid exists. B. S. Dandapat performed this work to obtain insight into the effect of viscosity, thermal conductivity, and thermocapillarity on the flow and the heat transfer rate. Dandapat's research allows to determine the flow and heat transfer characteristics of the fluids for different values of viscosity and thermal conductivity.

In B. S. Dandapat research, he obtained a system of ODEs through transformation technique. The system of ODEs is solved using the method of adjoints. He concluded that the dimensionless boundary layer thickness increases with the increase in viscosity of fluid while the free surface velocity decreases due to the thickening of liquid layer.

2.3 Effect of viscous dissipation on surface temperature:

R. C. Aziz [17] studied the viscous dissipation effect on surface temperature. Viscous dissipation is the process which involves heat generation due to the shear forces between adjacent layers of viscous fluid. He thoroughly studied the effects of viscous dissipation on free surface temperature of fluid. He then followed the scheme to transform PDEs to ODEs and then used the 10th order Homotopy analysis method (HAM) to investigate the effect of Eckert number on free surface temperature at different unsteadiness parameter and Prandtl number.

2.4 Effect of magnetic field and thermocapillarity on unsteady film flow:

N.F.M Noor and I. Hashim [18] researched the outcomes of thermocapillarity and magnetic field on unsteady thin film flow over the extending surface. The transformed ODEs were analytically solved using HAM. It was observed that when thermocapillarity number is increased in the absence of magnetic field the fluid speeds up after a slight deceleration while the fluid's temperature decreases regularly.

2.5 Effect of internal heating on an unsteady film flow:

R.C. Aziz et al. [19] studied an unsteady film flow over the extending surface with internal heating. The motion within the fluid and heat transfer arises solely due to the extending surface. He found out the effects of heat generation due to an internal source on flow velocity and temperature. He studied the effect of heat generation and absorption on the flow and heat transfer first by transforming the model into ODEs and then by solving the transformed ODEs using HAM. He reported that the heat generation or absorption had no effect on velocity due to the absence of this parameter in conservation of momentum equation.

2.6 Other researches:

Salleh et al. [20] performed a comprehensive study on boundary layer flow dynamics and the accompanying heat transfer mechanisms developed in the process when an extended sheet experiences Newtonian heating.

M. Megahed [21] applied the HPM to study the velocity, temperature, heat transfer rate, and the influence of slip velocity and variable heat flux on the skin friction coefficient in an unsteady boundary layer flow. Later, I-C Liu [22] in combination with A.M. Megahed analyzed the effect of thermal radiation and fluid property variation on flow and heat transfer. Liu's research used a numerical solution of the boundary layer flow problem, incorporating the influence of internal heat generation, variable heat flux, and thermal radiation. [23]

Different researchers investigated the time dependent film flow over the extending surface with distinct attributes, [24-26] with the purpose to help in creating better understanding of various phenomena with their work.

Elbashbeshy [27] presented a work on the heat transfer process taking place through a time dependent extending surface due to variable heat flux. The effect of a heat source or sink is accounted for in his analysis. He transformed the non-linear PDEs to non-line ODEs. Then, he employed the Runge-Kutta shooting method in order to solve the equations numerically.

Sakaidis [7] considered the characteristics of the boundary layer on a smooth flat plate issuing fluid at constant velocity through a slit within a stationary medium. He utilized two distinct approaches in his research to solve his model. The first approach entailed the numerical resolution of governing equations, which were transformed into a system of ODEs, whereas the second approach employed the integral method predicated on the presumed velocity profile. A favorable correlation among the methodologies was reported by him. Moreover, Sakaidis concluded that the drag force encountered by the sheet is significantly larger as compared with that experienced by a finite-length flat plate. As extension of Sakaidis's work, Crane [28] made a fundamental contribution in explaining the existence of a steady-state

solution for flow over an extending surface with velocity varying linearly along the distance from the slit.

Vleggaar [29] presented a comprehensive study on the behavior of laminar boundary-layer on continuous, accelerating surfaces. He solved the conservation equations (momentum and energy) in two reference frames i.e. rectangular and cylindrical with the help of similarity transformations in his study.

Motivated by the situation that often arises in the polymer processing industry, Gupta et al. [30] modified Crane's problem to include the effect of suction or blowing in a stretching sheet. He used similarity technique in his research. The temperature is assumed to be uniform parallel to its length in Crane's study but in practical life, this assumption doesn't work. Carragher et al. [31] reassessed Crane's study and put forward a similarity solution for the heat transfer process taking place through an extending surface at moderate and high Pr.

Jeng [32] conducted an extensive investigation into momentum and heat transfer phenomena occurring in a stretching sheet characterized by a changing velocity and a changing temperature distribution on its surface. His research resulted in solutions for both isothermal and non-isothermal surfaces. Furthermore, numerical examples with a power-law surface velocity and a linearly extending surface velocity along with a non-zero slit velocity were presented for the isothermal surface case. Kumeri et al.

[33] made the study even wider by analyzing the impact of the electrically conducting fluid on heat characteristics transfer of an extending sheet in a magnetic field, The observation indicated that the magnetic field augmented the rate of heat transfer under a specified surface temperature condition, whereas under a constant heat flux scenario, the surface temperature diminished as magnetic field intensity increased.

Grubka et al. [34] extended the investigation on power-law surface temperature fluctuations with regards to heat transfer as the researcher found a series of solution for the energy equation using Kummer's functions. Dutta et al. [35] obtained a temperature distribution for a sheet extending linearly, with uniform heat flux, while taking into consideration variable Prandtl numbers and concluded that at a given location, temperature is inversely dependent upon the Prandtl number.

Similarity transformation was used in each of the references listed above to transform the conservation equations into a framework of nonlinear ODEs. Lie point symmetry analysis tells us that if a differential equation possesses a Lie point symmetry, then we can use it to find new solutions to the equation from known solutions. First Lie point similarity is applied to transform the system of equation from a system of PDEs to a system of ODEs. Then different numerical methods are applied to solve the system in order to obtain the results.

Chapter 3: Methodology

Consider an unsteady 2D flow on a horizontal elastic sheet of uniform thickness $h(t)$, which propagates through a narrow slit as shown in Fig 3.1.

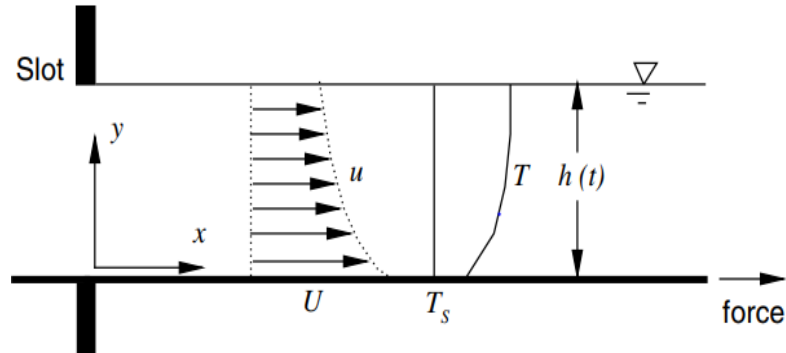


Figure 3.1: Schematic of flow through an extending surface

The flow over an unsteady surface with variable heat source or sink is represented by complex partial differential equations subjected to a few boundary conditions. In the first step, Lie symmetries of this model of non-linear partial differential equations are generated. This follows with the construction of invariants and the construction of reduced differential equations. As a result, a system of non-linear ordinary differential equations is obtained. The resulting system of ODEs is then solved using analytical method of HPM in this research study. All the coding is done on MAPLE software.

3.1 Lie symmetry

As mentioned in the previous chapter in section 2.1 that Wang studied the thin Newtonian film fluid on an unsteady extending surface and investigated the hydrodynamic behavior of this kind of flow numerically. Wang [12] used similarity transformation to transform system of non-linear PDEs to non-linear ODEs system. Whereas in this research, we employ Lie point symmetry technique to solve the system.

Lie point symmetry finds the solutions to a system of differential equations. The Lie point symmetries for the flow over an extending surface with variable heat source of sink can be found using the infinitesimals command in Maple package “PDEtools”.

3.2 Governing equations

We write our system of equations for the considered flow model with heat transfer on unsteady stretching surface along under the influence of variable heat source or sink shown in Figure 3.1 as:

$$\frac{\partial u}{\partial x} + \frac{\partial v}{\partial y} = 0, \quad (3.1)$$

$$\frac{\partial u}{\partial t} + u \frac{\partial u}{\partial x} + v \frac{\partial u}{\partial y} = \frac{\mu}{\rho} \frac{\partial^2 u}{\partial y^2}, \quad (3.2)$$

$$\frac{\partial T}{\partial t} + u \frac{\partial T}{\partial x} + v \frac{\partial T}{\partial y} - \frac{\kappa}{\rho c_p} \frac{\partial^2 T}{\partial y^2} - \frac{Q}{\rho c_p} (T - T_\infty) = 0. \quad (3.3)$$

Subjected to:

$$y = 0, u(x, t(0)) = U(x, t) = F_1(x, t), v(x, t(0)) = 0, \quad (3.4)$$

$$\kappa T_y(x, t(0)) = -q(x, t) = -F_2(x, t). \quad (3.4)$$

$$y = h(t), u(x, t(h(t))) = T(x, t(h(t))) = 0, v(x, t(h(t))) = \frac{dh}{dt}. \quad (3.5)$$

3.3 Generation of symmetries

The maple code for finding Lie point symmetries of above model of 3.1-3.3 subjected to 3.4 and 3.5 is given in Appendix. In the next step, symmetries of the model is generated as:

$$\begin{aligned} \mathbf{X} = & \xi_t(t, x, y, u, v, T) \frac{\partial}{\partial t} + \xi_x(t, x, y, u, v, T) \frac{\partial}{\partial x} + \xi_y(t, x, y, u, v, T) \frac{\partial}{\partial y} \\ & + \xi_u(t, x, y, u, v, T) \frac{\partial}{\partial u} + \xi_v(t, x, y, u, v, T) \frac{\partial}{\partial v} + \xi_T(t, x, y, u, v, T) \frac{\partial}{\partial T}, \end{aligned} \quad (3.6)$$

where ξ is called infinitesimal coordinate. The symmetries are generated using MAPLE software. The above model generates seven symmetries as given below:

$$\begin{aligned} \mathbf{X}_1 &= \frac{\partial}{\partial t}, \\ \mathbf{X}_2 &= \frac{\partial}{\partial x}, \\ \mathbf{X}_3 &= t \frac{\partial}{\partial x} + \frac{\partial}{\partial u}, \\ \mathbf{X}_4 &= x \frac{\partial}{\partial x} + u \frac{\partial}{\partial u}, \\ \mathbf{X}_5 &= (T - T_\infty) \frac{\partial}{\partial T}, \\ \mathbf{X}_6 &= e^{\frac{Qt}{\rho c_p}} \frac{\partial}{\partial T}, \\ \mathbf{X}_7 &= t \frac{\partial}{\partial t} + \frac{y}{2} \frac{\partial}{\partial y} - u \frac{\partial}{\partial u} - \frac{v}{2} \frac{\partial}{\partial v} + \frac{(T - T_\infty)Qt}{\rho c_p} \frac{\partial}{\partial T}. \end{aligned} \quad (3.7)$$

3.4 Construction of invariants:

The next step is to perform the reduction of the system by summing the symmetries that is $Z_1 = \sum_{i=1}^7 P_i X_i$. i.e.

$$Z_1 = P_1 X_1 + P_2 X_2 + P_3 X_3 + P_4 X_4 + P_5 X_5 + P_6 X_6 + P_7 X_7 . \quad (3.8)$$

It yields the following equations:

$$-(P_7 t + P_1)(F_1)_t - (P_3 t + P_4 x + P_2)(F_1)_x + P_4 u - P_7 u + P_3 = 0, \quad (3.9)$$

$$\frac{(P_7 t + P_1)(F_2)_t}{\kappa} + \frac{(P_3 t + P_4 x + P_2)(F_2)_x}{\kappa} + \frac{T_y(2P_7 Q t + 2P_5 \rho C_p - P_7 \rho C_p)}{2\rho C_p} = 0, \quad (3.10)$$

$$\frac{T_y(2P_7 Q t + 2P_5 \rho C_p - P_7 \rho C_p)}{2\rho C_p} = 0. \quad (3.11)$$

Invariants are required for the construction of similarity transformations. Invariants associated with Lie spanned by X_i , $i = 1 \dots 7$ is a function of independent and dependent variables of the system 3.1-3.5.

Invariants are obtained by employing an invariance criterion of the form $Z_1 \epsilon_1(t, x, y, u, v, T) = 0$ and solving the obtained linear partial differential equation.

The invariants associated with Z_1 are obtained through

$$Z_1 J(t, x, y, T, u, v) = 0 . \quad (3.12)$$

This leads to the generation of the system invariants that are equated to new independent r_1, r_2 and dependent W_1, W_2, W_3 variables as given below:

$$\begin{aligned} r_1 &= \frac{(P_7 t + P_1)^{\frac{P_4}{P_7}} (t P_3 P_4 + x P_4^2 - x P_4 P_7 + P_1 P_3 + P_2 P_4 - P_2 P_7)}{P_4 (P_4 - P_7)}, \\ r_2 &= \frac{y}{\sqrt{P_7 t + P_1}}, \\ W_1 &= \frac{(P_7 t + P_1)^{\frac{P_4}{P_7}} (u t P_4 P_7 - u t P_7^2 + t P_3 P_7 + u P_1 P_4 - u P_1 P_7 + P_1 P_3)}{(P_4 - P_7)}, \\ W_2 &= v \sqrt{P_7 t + P_1}, \end{aligned} \quad (3.13)$$

$$W_3 = \frac{(P_7 t + P_1)^{-\frac{P_5 \rho C_p + Q P_1}{P_7 \rho C_p}} (P_5 \rho C_p e^{\rho C_p (T_\infty - T)} + P_1 Q e^{\rho C_p (T - T_\infty)} - \rho C_p P_6) e^{-\frac{Q t}{\rho C_p}}}{-P_5 \rho C_p + Q P_1}.$$

3.5 Construction of reduced differential equation:

These transformations given in system of equations 3.13 map the system 3.1-3.3 to the below form in the form of independent r_1, r_2 and dependent W_1, W_2, W_3 variables.

$$W_{1,c_1} + W_{2,c_2} = 0, \quad (3.14)$$

$$(W_1 - P_4 r_1) W_{1,c_1} + (W_2 - \frac{P_7}{2} r_2) W_{2,c_2} + (P_4 - P_7) W_1 - \frac{\mu}{\rho} W_{1,c_2 c_2} = 0, \quad (3.15)$$

$$(W_1 - P_4 r_1) W_{3,c_1} + (W_2 - \frac{P_7}{2} r_2) W_{3,c_2} + (P_5 - \frac{Q P_1}{\rho C_p}) W_3 - \frac{\kappa}{3} W_{3,c_2 c_2} = 0. \quad (3.16)$$

Similarly the boundary conditions given in system 3.4 and 3.5 are written in the form of new independent and dependent variables as:

$$z_2 = 0, W_1(r_1, 0) = f_1(r_1), W_2(r_1, 0) = 0, W_3(r_1, 0) = -\frac{f_2(c_1)}{\kappa}. \quad (3.17)$$

$$z_2 = c_1, W_1(r_1, c_1) = W_3(r_1, c_1) = 0, W_2(r_1, c_1) = \frac{c_1 P_7}{2}. \quad (3.18)$$

3.6 Second reduction:

Now the same procedure is followed again in order to reduce the system of equations 3.14 to 3.18 further. In the first step, Lie symmetries of the system of equations 3.14 to 3.18 are generated. This follows with the construction of invariants and the construction of reduced differential equations. As a result, a system of non-linear ODEs is obtained.

The Lie symmetries are generated using MAPLE software. The above model generates two symmetries as given below:

$$X_8 = r_1 \frac{\partial}{\partial r_1} + W_1 \frac{\partial}{\partial W_1}, \quad (3.19)$$

$$X_9 = W_3 \frac{\partial}{\partial W_3}.$$

The next step is the summing of the symmetries that is $Z_2 = \sum_{i=8}^9 P_i X_i$ and then inserting it in $Z_2 \epsilon_2(r_1, r_2, W_1, W_2, W_3) = 0$. This will lead to invariants.

$$Z_2 = P_8 X_8 + P_9 X_9 . \quad (3.20)$$

Invariants are obtained by employing an invariance criterion of the form given below:

$$Z_2 J(r_1, r_2, W_1, W_2, W_3) = 0 . \quad (3.21)$$

This leads to the generation of the system invariants that are equated to new independent r and dependent P_1, P_2, P_3 variables as given below:

$$r = r_2 , \quad (3.22)$$

$$P_1 = \frac{W_1}{c_1} , \quad (3.23)$$

$$P_2 = W_2 , \quad (3.24)$$

$$P_3 = \frac{W_3}{c_1 \frac{P_8}{P_9}} . \quad (3.25)$$

These transformations mentioned above map the system of equation 3.14 to 3.16 to the below form in the form of independent r and dependent P_1, P_2, P_3 variables.

$$P_1 + P_2' = 0 , \quad (3.26)$$

$$P_1^2 - P_7 P_1 + (P_2 - P_7 \frac{c}{2}) P_1 - \frac{\mu}{\rho} P_1'' = 0 , \quad (3.27)$$

$$(P_5 - \frac{P_1 Q}{\rho} - \frac{P_4 P_9}{P_8}) P_3 + \frac{P_9}{P_8} P_1 P_3 + (P_2 - P_7 \frac{c}{2}) P_3' - \frac{\kappa}{\rho c_p} P_3'' = 0 . \quad (3.28)$$

The boundary conditions given in equations 3.17 and 3.18 are also transformed further to below form:

$$r = 0, P_1(0) = c_1, P_2(0) = 0, P_3(0) = -\frac{c_3}{\kappa} , \quad (3.29)$$

$$r = c_1, P_1'(c_1) = P_3'(c_1) = 0, P_2(c_1) = \frac{c_1 P_7}{2} . \quad (3.30)$$

The derivative is with respect to r in above equations. This system only involves parameters P_k , for $k = 6, 7, 8, 9$, which act and are claimed as the Lie control parameters because they are shown in the results here to control convergence of the analytic solution. There are no physical parameters yet involved, however these can be introduced by assuming

$$r = \beta \sqrt{\frac{\alpha \mu}{b \rho}} \eta, \quad (3.31)$$

$$P_1 = -\frac{b}{\alpha} f'(\eta), \quad (3.32)$$

$$P_2 = \beta \sqrt{\frac{\beta \mu}{\alpha \rho}} f(\eta), \quad (3.33)$$

$$P_3 = \frac{1}{\kappa} \sqrt{\frac{\mu}{b \rho}} \theta(\eta). \quad (3.34)$$

where α , b and β are constants. Using the above in the second reduced format of equations 3.26-3.28 of system of equations 3.1-3.3 and boundary conditions given in equations 3.4 and 3.5, we finally obtain a system and corresponding conditions with physical parameter and number, i.e., the Prandtl number Pr and the unsteadiness parameter S :

$$f''' + \beta^2 \left(\left(\frac{r_7}{2} S \eta - f \right) f'' + f'^2 + S P_7 f' \right) = 0, \quad (3.35)$$

$$\frac{\theta^{FF}}{Pr} + \beta^2 \left(\left(\frac{P_7}{2} S \eta - f \right) \theta' + \frac{P_9}{P_8} f' \theta - S \left(P_5 - \frac{Q P_1}{\rho c_p} - \frac{P_4 P_9}{P_8} \right) \theta \right) = 0. \quad (3.36)$$

Subjected to:

$$f'(0) = 1, f(0) = 0, \theta'(0) = 1, f''(1) = \theta'(1) = 0, f(1) = \frac{S}{2}. \quad (3.37)$$

where dot is a derivative with respect to similarity variables η . We have considered c_1 , c_2 and c_3 , to obtain the conditions written above, as:

$$c_1 = \frac{\beta}{P_7} \sqrt{\frac{\alpha \mu}{b \rho}}, \quad (3.38)$$

$$c_2 = -\frac{b}{\alpha}, \quad (3.39)$$

$$c_3 = -\sqrt{\frac{\mu}{b \rho}}. \quad (3.40)$$

3.7 Homotopy perturbation method (HPM)

In this study, an analytical solution method known as Homotopy perturbation method is used to find out the solution of the model of flow through a non-uniform stretching surface.

The Homotopy perturbation method is an extraordinary analytical technique used to tackle many linear and nonlinear ordinary and partial differential equations. It combines two ideas, i.e. perturbation and Homotopy. In the perturbation method, a small change is introduced to a known solution and then afterward deriving a new solution by using those changes. While Homotopy is a continuous transformation between two mathematical functions. Solutions developed with perturbation techniques are easily affected by a small parameter that a small change in the small parameter changes the results. HPM provides the solution by requiring the initial conditions only. In this way, it is highly advantageous to use HPM as it is an efficient and effective technique used to solve complex ordinary and partial differential equations.

In HPM, the equations are expressed as a power series as given below:

$$f(\eta) = f_0(\eta) + pf_1(\eta) + p^2f_2(\eta) + p^3f_3(\eta) + \dots + p^n f_n(\eta), \quad (3.41)$$

$$\theta(\eta) = \theta_0(\eta) + p\theta_1(\eta) + p^2\theta_2(\eta) + p^3\theta_3(\eta) + \dots + p^n \theta_n(\eta), \quad (3.42)$$

$$\gamma = \gamma_0 + p\gamma_1 + p^2\gamma_2 + p^3\gamma_3 + \dots + p^n \gamma_n, \quad (3.43)$$

$$f'''(\eta) = f_0'''(\eta) + pf_1'''(\eta) + p^2f_2'''(\eta) + \dots + p^n f_n'''(\eta), \quad (3.44)$$

$$f''(\eta) = f_0''(\eta) + pf_1''(\eta) + p^2f_2''(\eta) + \dots + p^n f_n''(\eta), \quad (3.45)$$

$$\begin{aligned} f(\eta)f''(\eta) &= [f_0(\eta) + pf_1(\eta) + p^2f_2(\eta) + \dots + p^n f_n(\eta)][f_0''(\eta) + pf_1''(\eta) + p^2f_2''(\eta) + \dots \\ &\quad + p^n f_n''(\eta)], \\ &= f_0(\eta)f_0''(\eta) + p(f_1(\eta)f_0''(\eta) + f_0(\eta)f_1''(\eta)) + p^2(f_2(\eta)f_0''(\eta) + \\ &\quad f_1(\eta)f_1''(\eta) + f_0(\eta)f_2''(\eta)) . \end{aligned} \quad (3.46)$$

In the above power series, it can be seen that a parameter p is multiplied. So in HPM a small parameter is introduced i.e. a small change is introduced to a known solution and then afterward deriving a new solution by using those changes.

In order to solve system 3.35 and 3.36 using HPM, the basic nomenclature is:

$$(1 - p)f'''' + p(f'''' + \beta^2((\frac{P_7}{2}S\eta - f)f'' + f'^2 + SP_7f')) = 0, \quad (3.47)$$

$$(1 - p)\theta'' + p\left(\frac{\theta^{FF}}{Pr} + \beta^2\left(\frac{P_7}{2}S\eta - f\right)\theta' + \frac{P_9}{P_8}f'\theta - S\left(\frac{P}{5} - \frac{QP^1}{P_8} - \frac{P^4P_9}{P_8}\right)\theta\right) = 0. \quad (3.48)$$

The power series expression given in 3.41 to 3.46 are to be inserted in equations 3.47 and 3.48. By equating the terms with the same power of the parameter p , we get a system of linear ODEs. As already mentioned in HPM, initial conditions are required.

In our system of initial conditions given in 3.37, $f''(0)$ is not given. Similarly, $\theta(0)$ is not given. So in HPM, these are assumed as α and ε respectively.

$$f(0) = 0, f'(0) = 1, f''(0) = \alpha, \quad (3.49)$$

$$\theta(0) = \varepsilon, \theta'(0) = 1. \quad (3.50)$$

By equating the terms with the same power of the parameter p in equation 3.47, we get a system of linear ODEs and then substituting the initial values given in 3.49, we get the value of $f_0, f_1, f_2, \dots, f_n$. Similarly, by equating the terms with the same power of the parameter p in equation 3.48, we get a system of linear ODEs and then substituting the initial values given in 3.50, we get the value of $\theta_0, \theta_1, \theta_2, \dots, \theta_n$.

It should be noted that the values of α, γ and ε are unknowns and their values are to be determined. These values can be found out by using the outer boundary conditions given in 3.37 that are not being used yet i.e.

$$f''(1) = \theta'(1) = 0, f(1) = \frac{S}{2}. \quad (3.51)$$

In this study, we have found the solution using 10th order approximations for both $f(\eta)$ and $\theta(\eta)$. The system of ordinary differential equations given in 3.35 and 3.36 depends on various parameters, such as the unsteadiness parameter, the Prandtl number, and six additional control parameters i.e. P_4, P_5, P_7, P_8, P_9 and P_{10} . The Maple code for finding the solution using HPM is given in Appendix.

Chapter 4: Results

In the previous chapter, we employed Lie similarity transformation technique to obtain ODEs corresponding to flow equations. The system of ODEs is mentioned in equations 3.47 and 3.48. These ODEs are subjected to initial conditions given in equations 3.49 and 3.50 and boundary condition 3.51. The system of ODEs is solved by writing code for Homotopy perturbation method on MAPLE. The system of ODEs is solved by applying 10th order HPM. The MAPLE code is composed in such a way that the order of solution could be increased or decreased by simply changing the value of 'n' in the program where n denotes the order of HPM.

With increasing the order, the results become more precise along with increased computational time. Generally, the HPM model solved at order 7 shows results consistent with order 15. The HPM model under study is also solved on 15th order as well. It shows result consistent with order 10th. So in this research, the results are obtained at order 10th. The velocity and temperature profiles are obtained at this order to determine the solution.

Our system of odes depends on different parameters which include unsteadiness parameter, Prandtl number, and six additional control parameters i.e.

P_4 , P_5 , P_7 , P_8 , P_9 and P_{10} . Each of these parameters has its own effect on velocity profile $f'(\eta)$ and temperature profile $\theta(\eta)$. We keep changing the value of each of these parameters one by one to observe the velocity profile $f'(\eta)$ and temperature profile $\theta(\eta)$. Now let's consider each of these parameters one by one in the subsequent sections.

4.1 Influence of unsteadiness parameter 'S'

Firstly, the velocity profiles $f'(\eta)$ and temperature profiles $\theta(\eta)$ for different values of unsteadiness parameter S are drawn by keeping all other parameters constant. Both the profiles are greatly dependent on the value of S . We obtain the desired profiles on the certain values of S . The desired profile which is increasing trend is obtained for unsteadiness values greater than 2.

Now first see the influence of unsteadiness parameter S on velocity $f'(\eta)$. The variation of unsteadiness parameter on the velocity profile is measured and shown graphically in Figure 4.1. It shows that the velocity rises with the increase in the value of S while keeping all other parameters including Prandtl number, and six other control parameters constant. So increasing trend is obtained in case of velocity profiles while varying the value of S .

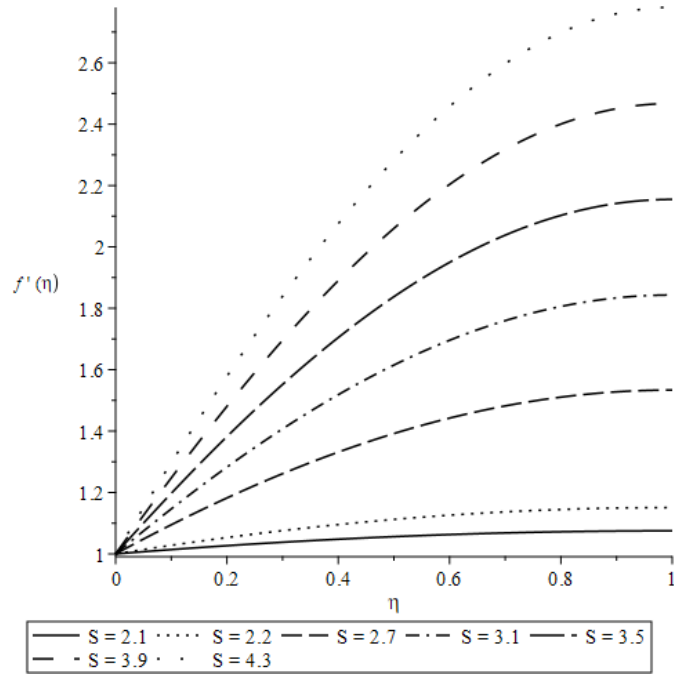


Figure 4.1: Variation of $f'(\eta)$ with S ($Pr = 1, \vartheta_4 = \vartheta_5 = \vartheta_7 = \vartheta_8 = \vartheta_{10} = 1, \vartheta_9 = 2.5$)

In the same manner the variation of S is measured on the $\theta(\eta)$ after obtaining the velocity profile. The temperature profile $\theta(\eta)$ is shown in Figure 4.2:

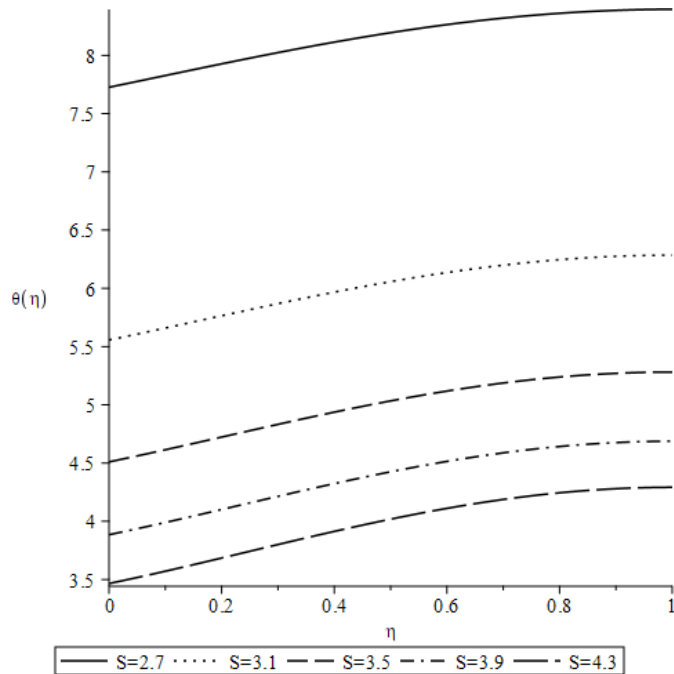


Figure 4.2: Variation of $\theta(\eta)$ with S ($Pr = 1, \vartheta_4 = \vartheta_5 = \vartheta_7 = \vartheta_8 = \vartheta_{10} = 1, \vartheta_9 = 2.5$)

The variation of unsteadiness parameter S on the $\theta(\eta)$ shows that as the value of S continues to increase, the temperature curve moves down towards the origin. So it

means that the temperature value is decreasing with the increase in value of S . The Figure 4.2 shows that initially with an increase in the value of S from 2.7 to 3.1, there is a big gap in between two curves. But later on, this gap becomes smaller between the two neighboring curves. So it means that with the increase in value of S the temperature initially decreases significantly but afterwards there is gradual decrease in temperature value.

The influence of S on the velocity and temperature profile is further explained in the Table 4.1 while keeping all remaining parameters constant. The table exhibits the influence of S on the dimensionless film thickness β , velocity gradient $f'(1)$ and free surface temperature $\theta(1)$. It can be seen that the unsteadiness factor plays a vital role on the dimensionless film thickness β , velocity gradient $f'(1)$ and free surface temperature $\theta(1)$. The β rises with the rise in S till S equals to 3.9 but after that β starts decreasing with further rise in S , which is evident from the Table 4.1 as well.

Table 4.1: Variation of dimensionless film thickness, velocity gradient and free surface temperature with respect to S

S	β	α	$f'(1)$	ϵ	$\theta(1)$
2.7	0.4219431846	0.982636784	1.533695073	7.72605554	8.394826316
3.1	0.4535705456	1.509588421	1.843321387	5.55658533	6.284609387
3.5	0.4632735864	2.024574106	2.154649721	4.51017539	5.280909425
3.9	0.4631288220	2.532194990	2.467055560	3.88510111	4.687269360
4.3	0.4582065692	3.035032121	2.780177484	3.03503212	4.291835535
4.7	0.4509257442	3.534622300	3.093794888	3.16408656	4.008022340
5.1	0.4425306311	4.031926879	3.407766936	2.93554445	3.793654826

In the previous chapter, $f''(0)$ and $\theta(0)$ were assumed to α and ϵ respectively. So α is equal to $f''(0)$ and ϵ is equal to $\theta(0)$. The table indicates that the velocity gradient $f'(1)$ and α are increasing with the S . Similarly, the free surface temperature $\theta(1)$ and ϵ are decreasing as S increases. This is in agreement with Figure 4.1 and Figure 4.2 i.e. the velocity profile moves upward away from the origin with increasing unsteadiness parameter and temperature profile moves downward towards the origin with increasing unsteadiness parameter.

4.2 Influence of Prandtl number 'Pr'

As unsteadiness parameter affects the model, Prandtl Number is another parameter that influences the model. Velocity profile remains unaffected by varying the Prandtl number. It can be noticed through equation 3.35. As it does not contain Prandtl number. While equation 3.36 has Prandtl number so the temperature profile depends greatly on Prandtl Number.

There is an inverse relation between Pr and $\theta(\eta)$. With the increase in Pr the temperature decreases. Initially a bigger decrease is observed with the increase in Pr .

But on further rise in the Pr, the gap between the decreasing temperature profiles also becomes smaller. So it means that the temperature is observing smaller decrement on greater Prandtl numbers.

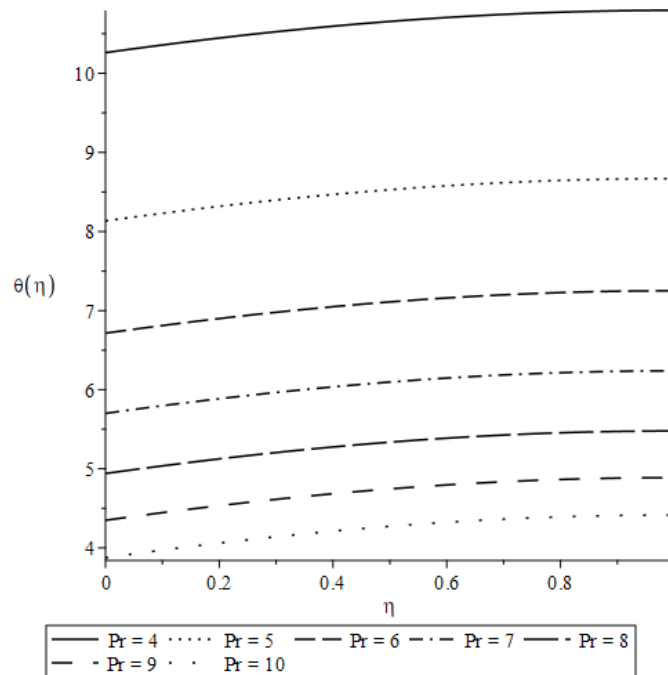


Figure 4.3: Variation of $\theta(\eta)$ with Pr ($S = 2.1, \vartheta_4 = \vartheta_5 = \vartheta_7 = \vartheta_8 = \vartheta_{10} = 1, \vartheta_9 = 2.5$)

The influence of Pr on the $\theta(\eta)$ is further explained in the Table 4.2. The table exhibits the influence of Pr on the β , free surface temperature $\theta(1)$ and $\theta(0)$. It is noted that the Prandtl Number plays an important role in determining the temperature profile. The film thickness β remains constant on different values of Pr, which is evident from the Table 4.2 as well. So the β is independent of Pr number.

Table 4.2: Variation of dimensionless film thickness and free surface temperature with respect to Pr

Pr	β	ϵ	$\theta(1)$
1	0.2115871341	42.17261756	42.70353445
2	0.2115871341	20.89889093	21.43077971
3	0.2115871341	13.80727449	14.34013957
4	0.2115871341	10.26118377	10.79502962
5	0.2115871341	8.133301844	8.668132914
6	0.2115871341	6.714523077	7.250343876
7	0.2115871341	5.700945054	6.237760117
8	0.2115871341	4.940616539	5.478430433
9	0.2115871341	4.349120165	4.887937489
10	0.2115871341	3.875805529	4.415630915

The table indicates that the free surface temperature $\theta(1)$ and ε are decreasing when Prandtl number rises. This is in agreement with Figure 4.3 i.e. the temperature profile moves downward with increasing of Pr .

The Figure 4.3 and Table 4.2 are given for unsteadiness parameter S equal to 2.1. Now we change the value of S to 2.7 and then see the influence of Pr on $\theta(\eta)$. The resulting profile is given in Figure 4.4. It shows that the temperature profiles are moving further closer to origin in case of S equals to 2.7 as compared to S of 2.1 given in Figure 4.3.

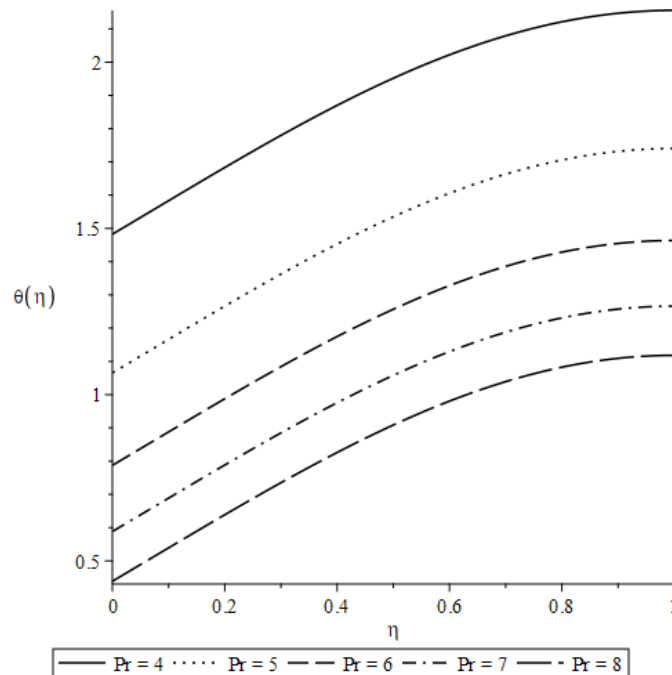


Figure 4.4: Variation of $\theta(\eta)$ with Pr ($S = 2.7$, $\lambda_4 = \lambda_5 = \lambda_7 = \lambda_8 = \lambda_{10} = 1$, $\lambda_9 = 2.5$)

As the unsteadiness parameter has inverse relation with the temperature value. That is why, the temperature profile has moved further downward in Figure 4.4 as compared to Figure 4.3.

In the same manner, temperature profiles are drawn for different Pr number while varying S equal to 3.1, 3.5, 3.9 and 4.3 in Figure 4.5, Figure 4.6, Figure 4.7 and Figure 4.8 respectively. In all of these profiles, as S is increasing the temperature profiles are moving closer to the origin. It means that the temperature is decreasing.

It is also noticeable that with increasing Pr , the gaps between the temperature profiles become narrower. For S equals to 3.5, the temperature profile is moving below the origin when Pr number equals to 8 which is not an optimum profile that is why it is omitted in Figure 4.6.

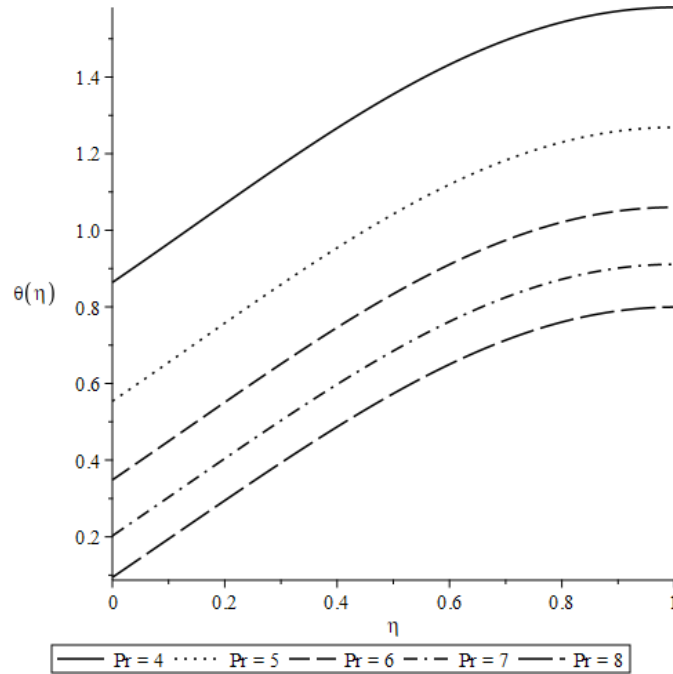


Figure 4.5: Variation of $\theta(\eta)$ with Pr ($S = 3.1$, $\vartheta_4 = \vartheta_5 = \vartheta_7 = \vartheta_8 = \vartheta_{10} = 1$, $\vartheta_9 = 2.5$)

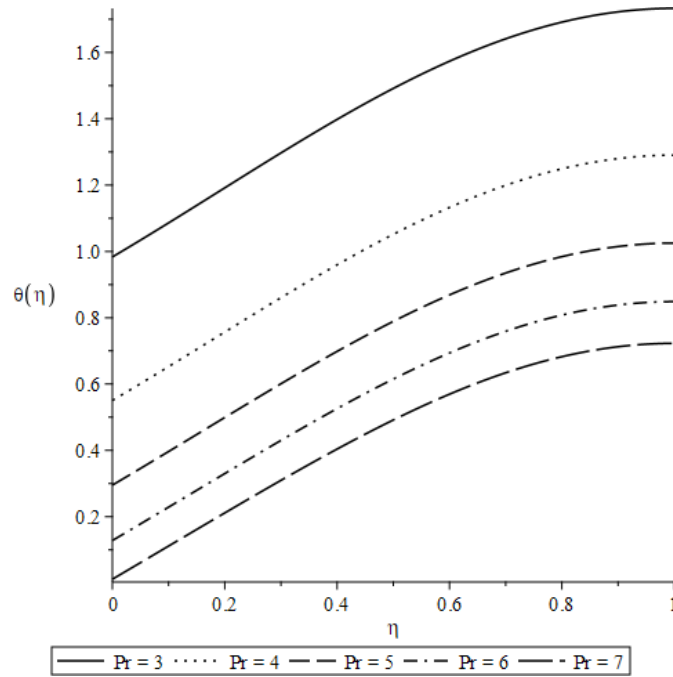


Figure 4.6: Variation of $\theta(\eta)$ with Pr ($S = 3.5$, $\vartheta_4 = \vartheta_5 = \vartheta_7 = \vartheta_8 = \vartheta_{10} = 1$, $\vartheta_9 = 2.5$)

Similarly for the unsteadiness parameter of 3.9 and 4.3, Pr number of 6 and greater are omitted in Figure 4.7 and Figure 4.8 as the temperature profile moves down the origin for these values of Pr which are not optimum profiles. For all these temperature

profiles, it is evident that with the increase in Pr and S, the temperature decreases, and temperature profile moves further closer to origin.

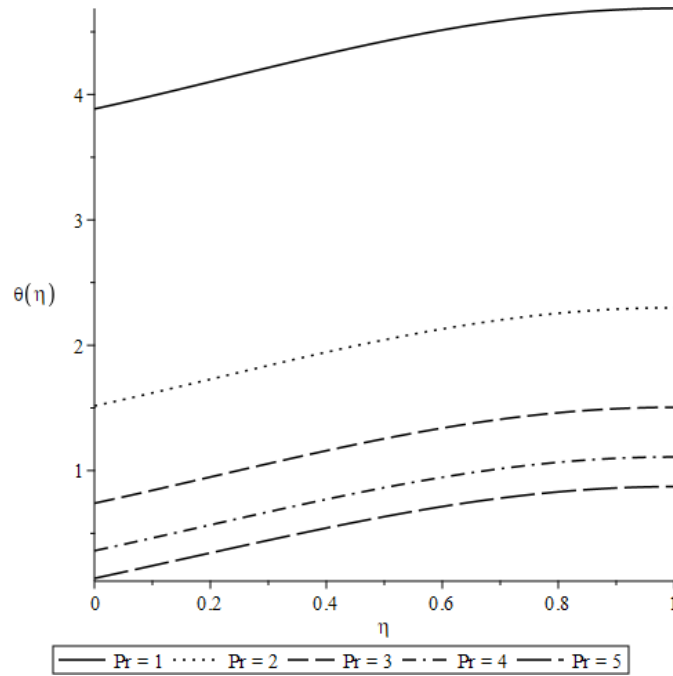


Figure 4.7: Variation of $\theta(\eta)$ with Pr ($S = 3.9$, $\vartheta_4 = \vartheta_5 = \vartheta_7 = \vartheta_8 = \vartheta_{10} = 1$, $\vartheta_9 = 2.5$)

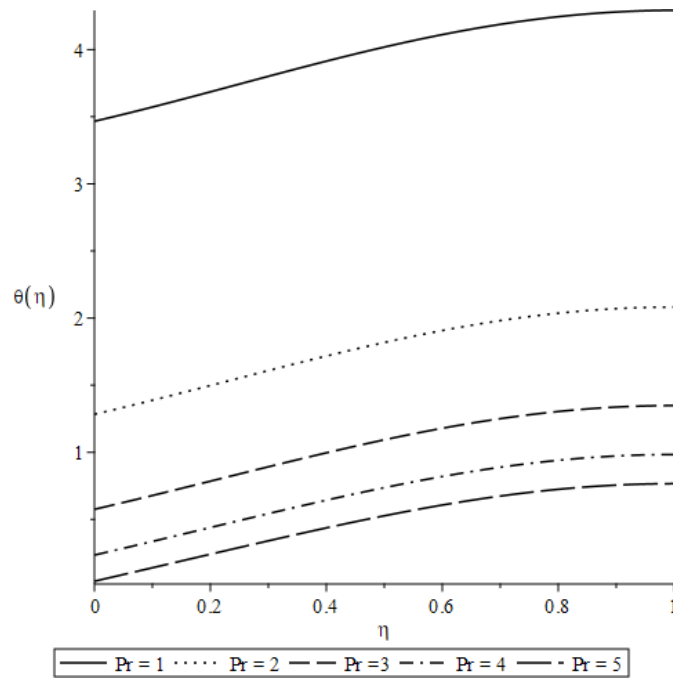


Figure 4.8: Variation of $\theta(\eta)$ with Pr ($S = 4.3$, $\vartheta_4 = \vartheta_5 = \vartheta_7 = \vartheta_8 = \vartheta_{10} = 1$, $\vartheta_9 = 2.5$)

4.3 Influence of control parameters

In this study model, there are six control parameters that determines the solution of the complex problem of flow over an unsteady stretching surface. These parameters have tremendous influence on the solution.

The control parameters are P_4 , P_5 , P_7 , P_8 , P_9 and P_{10} . Now we will look at them one by one to see their influence on the solution.

4.3.1 Influence of P_4 , P_5 and P_{10}

As equation 3.35 describes the velocity profile, it can be seen that equation 3.35 does not contain P_4 , P_5 and P_{10} . So P_4 , P_5 and P_{10} have no influence on the velocity profile of the model. While equation 3.36, which describes the temperature profile, contains these control parameters P_4 , P_5 and P_{10} . But it is observed through Maple results that the P_4 , P_5 and P_{10} does not affect the temperature profile as well. It means that the model remains unaffected by these three control parameters i.e. P_4 , P_5 and P_{10} .

4.3.2 Influence of P_9

Velocity profile is independent of the value of P_9 , as equation 3.35 does not contain P_9 . The temperature profile is hugely dependent on the control parameter P_9 . There are certain values of P_9 at which an optimum solution is obtained. The desired profile is obtained for P_9 greater than 2.05 and less than 53.

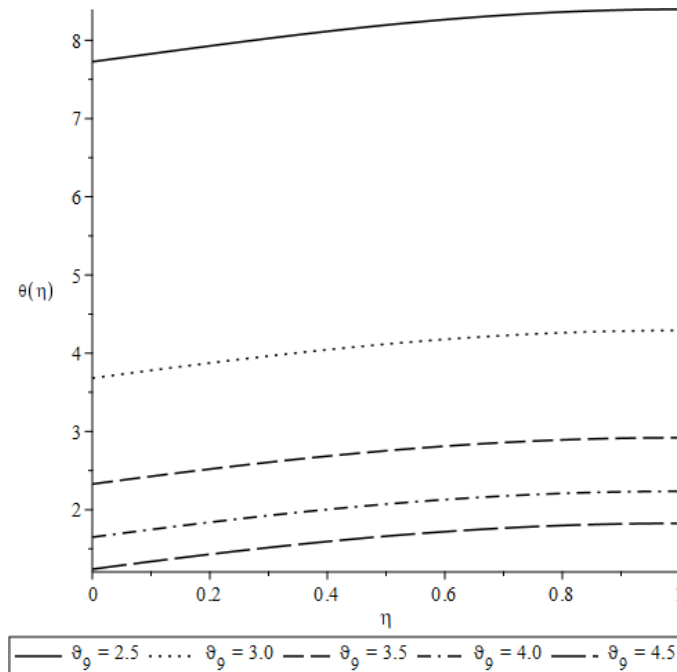


Figure 4.9: Variation of $\theta(\eta)$ with θ_9 ($S = 2.7$, $\theta_4 = \theta_5 = \theta_7 = \theta_8 = \theta_{10} = 1$, $Pr = 1$)

As P_9 rises, the temperature decreases. Initially while increasing the P_9 , there is a big decrease in the temperature $\theta(\eta)$. But on further increase in P_9 , the temperature decreases slowly as seen from Figure 4.9. It is noticeable that there is a great difference between P_9 value of 2.5 and 3.0. While on the further increase in P_9 , there is gradual decrease in temperature profile.

The influence of P_9 value on the $\theta(\eta)$ is further explained in Table 4.3. The table exhibits the influence of P_9 value on the β , $\theta(1)$ and $\theta(0)$. It can be seen that the P_9 plays an important role in determining the temperature profile. The β remains constant on different values of P_9 , which is evident from Table 4.3 as well. So β is independent of P_9 .

Table 4.3: Variation of dimensionless film thickness and free surface temperature with respect to ϑ_9

P_9	β	ε	$\theta(1)$
2.5	0.4219431846	7.726055541	8.394826316
3.0	0.4219431846	3.681232124	4.289813466
3.5	0.4219431846	2.327417576	2.919484512
4.0	0.4219431846	1.648281365	2.234883480
4.5	0.4219431846	1.239289794	1.824935066
5.0	0.4219431846	0.9654201059	1.552436625
5.5	0.4219431846	0.7687604709	1.358544589
6.0	0.4219431846	0.6203392009	1.213824145
6.5	0.4219431846	0.5040538054	1.101918253
7.0	0.4219431846	0.4102388370	1.013011395

The above table indicates that the free surface temperature $\theta(1)$ and ε are decreasing as the P_9 increases. This is in agreement with Figure 4.9 i.e. the temperature profile moves downward with increasing value of control parameter P_9 .

The Figure 4.9 and Table 4.3 are given for unsteadiness parameter equals to 2.7. It is evident from the Table 4.3 that there is a significant decrease in the temperature as P_9 increases from 2.5 to 3.0. On the further increase in P_9 , the decrease in temperature becomes lesser.

Now we change S and then see the influence of P_9 on $\theta(\eta)$. The profile for S equals 2.1 is shown in Figure 4.10. It shows that the temperature profiles are moving further closer to origin in case of S equals to 2.7 given in Figure 4.9 as compared to S equals to 2.1 given in Figure 4.10.

P_9 is the most important control parameter. It has almost same influence as that of unsteadiness parameter for the temperature profiles. In both cases, temperature decreases with the increase in their respective values. When both unsteadiness parameter and P_9 increases, the temperature profile moves further closer to the origin.

This is evident from Figures 4.9 to 4.15, in which variation of $\theta(\eta)$ with λ_9 at variable values of S is graphically plotted.

In Figure 4.10 and 4.11, S decreased to 2.1 and 2.2 respectively and it can be seen that temperature values are greater than the case of Table 4.3 in which S was considered as 2.7.

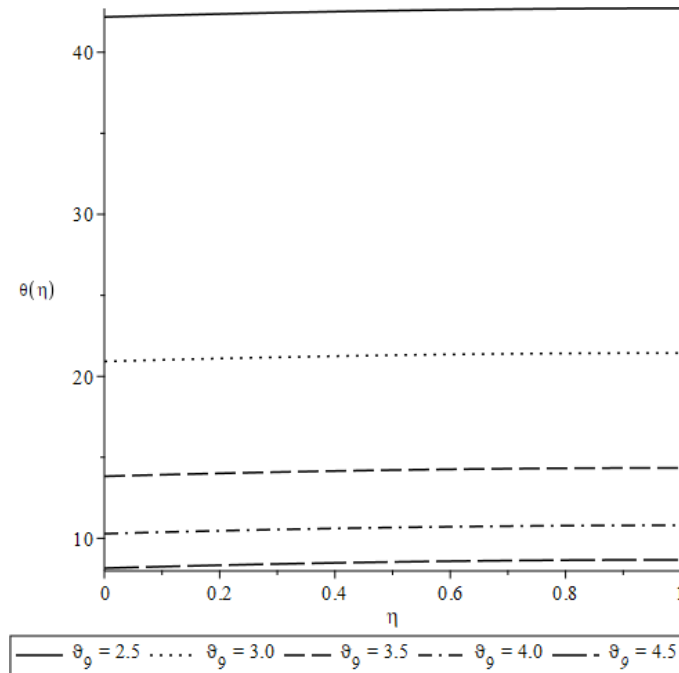


Figure 4.10: Variation of $\theta(\eta)$ with ϑ_9 ($S = 2.1$, $\vartheta_4 = \vartheta_5 = \vartheta_7 = \vartheta_8 = \vartheta_{10} = 1$, $Pr = 1$)

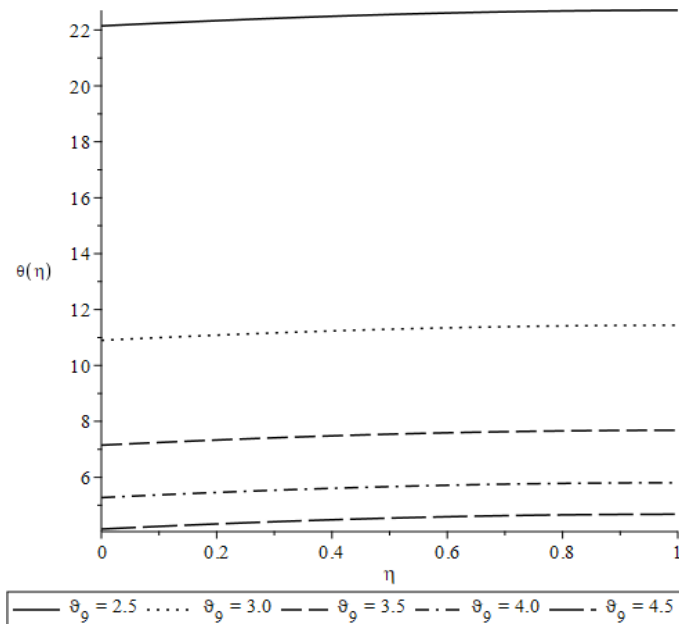


Figure 4. 11: Variation of $\theta(\eta)$ with ϑ_9 ($S = 2.2$, $\vartheta_4 = \vartheta_5 = \vartheta_7 = \vartheta_8 = \vartheta_{10} = 1$, $Pr = 1$)

It is noticeable that with increasing P_9 , the gaps between the temperature profiles become narrower. In Figure 4.12, observe the difference in temperature profiles at different values of λ_9 . It can be seen that gaps in temperature profiles become narrower with increase in P_9 .

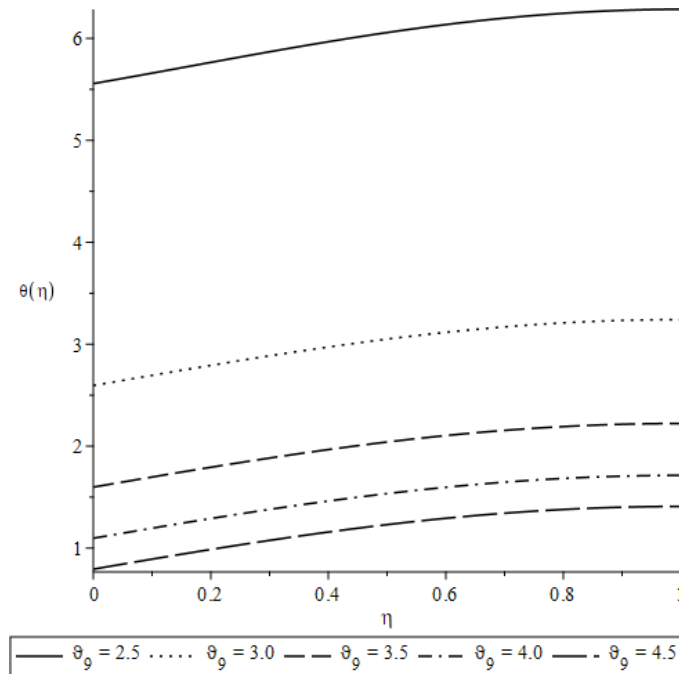


Figure 4. 12: Variation of $\theta(\eta)$ with ϑ_9 ($S = 3.1, \vartheta_4 = \vartheta_5 = \vartheta_7 = \vartheta_8 = \vartheta_{10} = 1, Pr = 1$)

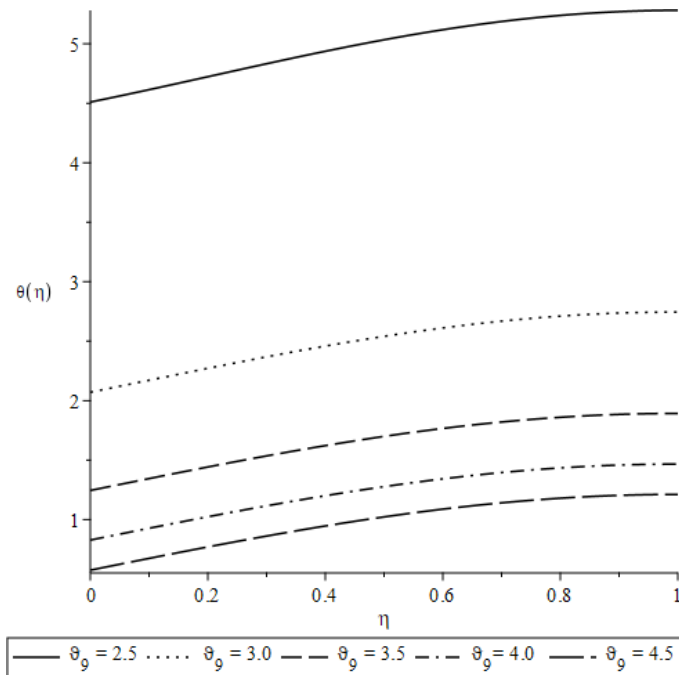


Figure 4. 13: Variation of $\theta(\eta)$ with ϑ_9 ($S = 3.5, \vartheta_4 = \vartheta_5 = \vartheta_7 = \vartheta_8 = \vartheta_{10} = 1, Pr = 1$)

In Figures 4.13, 4.14 and 4.15, same trend is observed i.e. with increase in P_9 , the temperature decreases. Furthermore, it can again be seen from these profiles that with rise in S , the temperature is decreasing further.

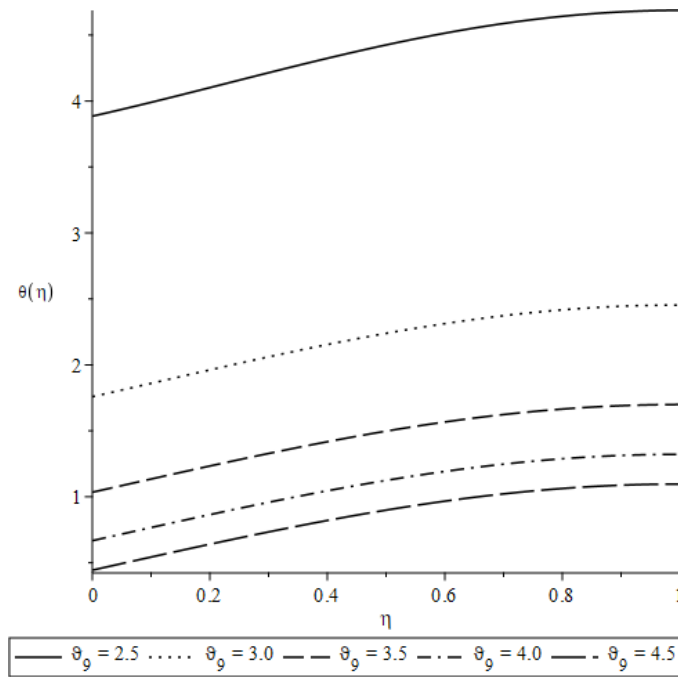


Figure 4.14: Variation of $\theta(\eta)$ with ϑ_9 ($S = 3.9$, $\vartheta_4 = \vartheta_5 = \vartheta_7 = \vartheta_8 = \vartheta_{10} = 1$, $Pr = 1$)

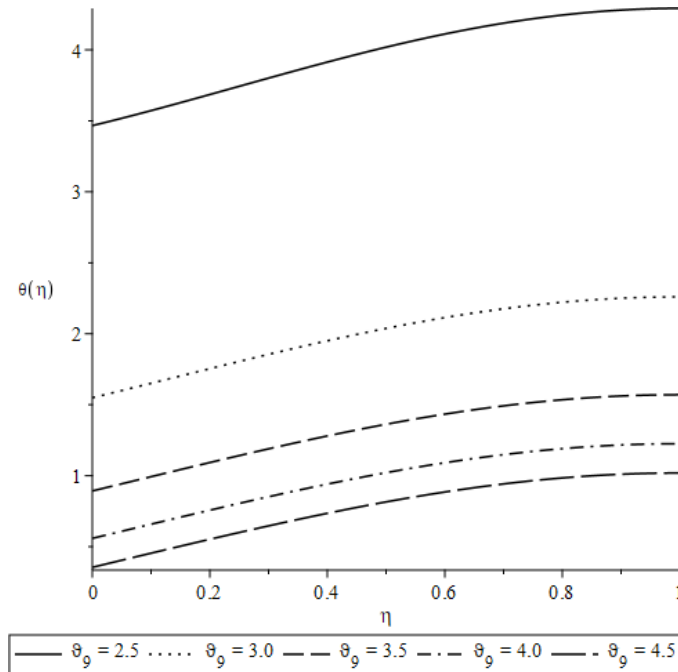


Figure 4.15: Variation of $\theta(\eta)$ with ϑ_9 ($S = 4.3$, $\vartheta_4 = \vartheta_5 = \vartheta_7 = \vartheta_8 = \vartheta_{10} = 1$, $Pr = 1$)

4.3.3 Influence of P_7

P_7 is an important control parameter that influences both the velocity profiles and temperature profiles. Equation 3.35 and 3.36, both contain P_7 , so both the profiles show variation with the change in P_7 value. But there is only a small range of values of P_7 where optimum velocity and temperature profiles are obtained.

The optimum profile is obtained for P_7 value between 0.12 and 1.89 for unsteadiness value of 2.7. Similarly, the optimum profile range changes slightly with change in the unsteadiness parameter and other control parameters. With the rise in the P_7 , the velocity profile moves towards the origin i.e. velocity starts decreasing with rise in P_7 . But there is very small difference in the velocities. This is evident from Figure 4.16, in which variation of velocity is shown with respect to the P_7 while keeping all other parameters constant.

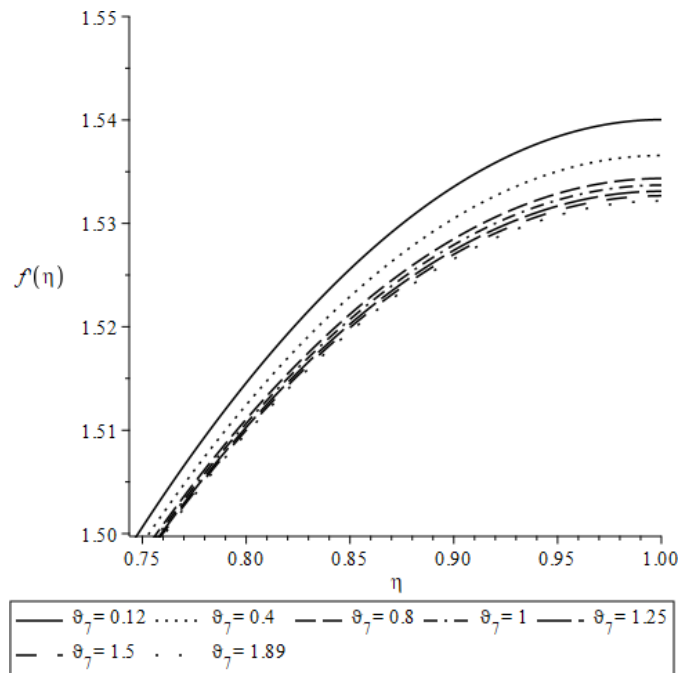


Figure 4. 16: Variation of $f'(\eta)$ with ϑ_7 ($S = 2.7, \vartheta_4 = \vartheta_5 = \vartheta_8 = \vartheta_{10} = 1, \vartheta_9 = 2.5, Pr = 1$)

The P_7 also affects the temperature profile. With the increase in P_7 , the temperature profile moves upward away from the origin, which means the temperature value is increasing. It is evident from the Figure 4.17(a) and Figure 4.17(b) that $\theta(\eta)$ moves uniformly upwards with the increase in P_7 . In the second Figure below, it can be seen that the two temperature profiles are separated by the same distance.

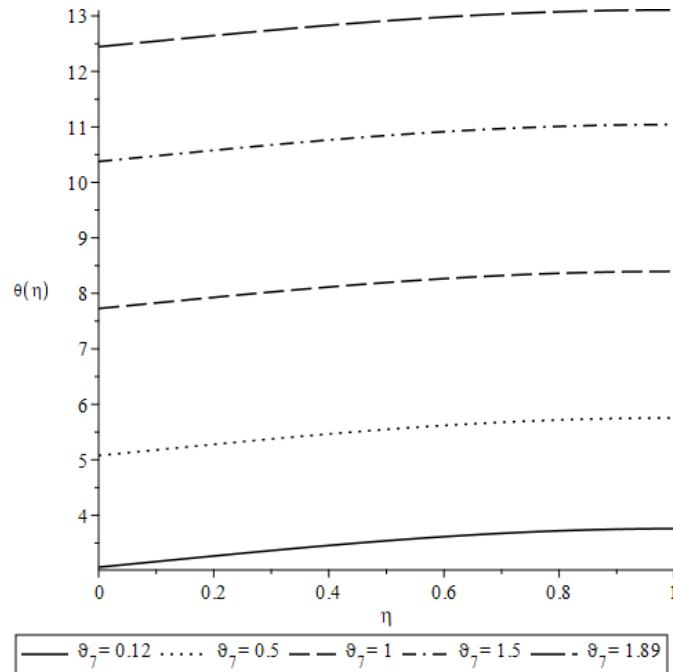


Figure 4. 17(a): Variation of $\theta(\eta)$ with λ_7 ($S = 2.7$, $\vartheta_4 = \vartheta_5 = \vartheta_8 = \vartheta_{10} = 1$, $\vartheta_9 = 2.5$, $Pr = 1$)

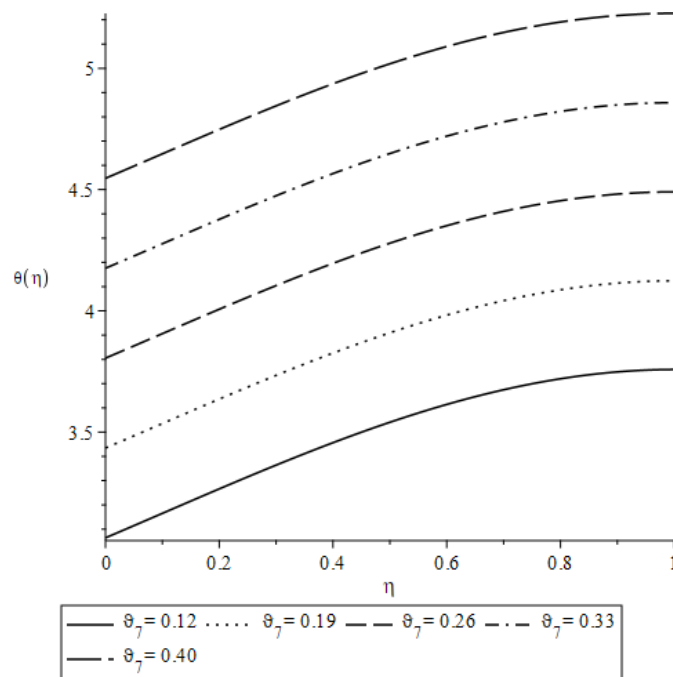


Figure 4. 17(b): Variation of $\theta(\eta)$ with λ_7 ($S = 2.7$, $\vartheta_4 = \vartheta_5 = \vartheta_8 = \vartheta_{10} = 1$, $\vartheta_9 = 2.5$, $Pr = 1$)

The two figures are shown for the variation of temperature profile with P_7 in Figure 4.17(a) and 4.17(b). In first Figure, the temperature profile looks like a straight line. This is due to the fact that a greater range of values are taken in this case. But in actual

these are curves instead of straight line. This can be seen in the Figure 4.17(b), instead of straight lines, curves are obtained as smaller range of values are considered in it.

The influence of P_7 on the velocity and $\theta(\eta)$ is further explained in the Table 4.4. The table exhibits the influence of P_7 on the dimensionless film thickness β , velocity gradient $f'(1)$ and free surface temperature $\theta(1)$. It can be seen that P_7 plays a vital role on the values of dimensionless film thickness β , velocity gradient $f'(1)$ and free surface temperature $\theta(1)$. The dimensionless film thickness β decreases with the rise in value of P_7 as evident from the Table 4.4. It can be seen that initially with the increase in P_7 , there is a greater decrease in dimensionless film thickness. But on further increase, it decreases lesser as compared to the previous case.

Table 4.4: Variation of dimensionless film thickness, velocity gradient and free surface temperature with respect to ϑ_7

P_7	β	α	$f'(1)$	ϵ	$\theta(1)$
0.2	0.6340336099	0.9650840140	1.538722547	3.48744933	4.176125582
0.4	0.5528523380	0.9725329663	1.536560076	4.54652202	5.226558861
0.6	0.4966454155	0.9771700815	1.535235674	5.60615110	6.280955044
0.8	0.4547434171	0.9803365265	1.534340627	6.66603491	7.337326788
1.0	0.4219431846	0.9826367844	1.533695073	7.72605554	8.394826315
1.2	0.3953598681	0.9843837514	1.533207378	8.78615778	9.453030514
1.4	0.3732467376	0.9857557323	1.532825913	9.84631230	10.51170434
1.6	0.3544756190	0.9868618145	1.532519360	10.9065030	11.57070752
1.8	0.3382808379	0.9877724970	1.532267617	11.9667187	12.62994974

In the previous chapter, $f''(0)$ and $\theta(0)$ were assumed to α and ϵ respectively. So α is equal to $f''(0)$ and ϵ is equal to $\theta(0)$. The above table indicates that the velocity gradient $f'(1)$ is decreasing very little with the increase of P_7 value. While the free surface temperature $\theta(1)$ and ϵ are increasing uniformly as the P_7 value increases. This is in agreement with Figure 4.16 and Figure 4.17 i.e. the velocity profile is almost constant and moves toward origin with increasing P_7 and temperature profile moves uniformly upward with increasing P_7 .

4.3.4 Influence of P_8

Velocity profile is independent of the value of P_8 , as equation 3.35 does not contain P_8 . The temperature profile is dependent on the control parameter P_8 . There are certain values of P_8 at which optimum temperature profiles are obtained. The desired profile is obtained for P_8 greater than 0.225 and less than 1.25 for unsteadiness parameter value of 2.7. So the optimum value varies depending on the values of other parameters as well. Figure 4.18 describes the variation of P_8 on the temperature profile.

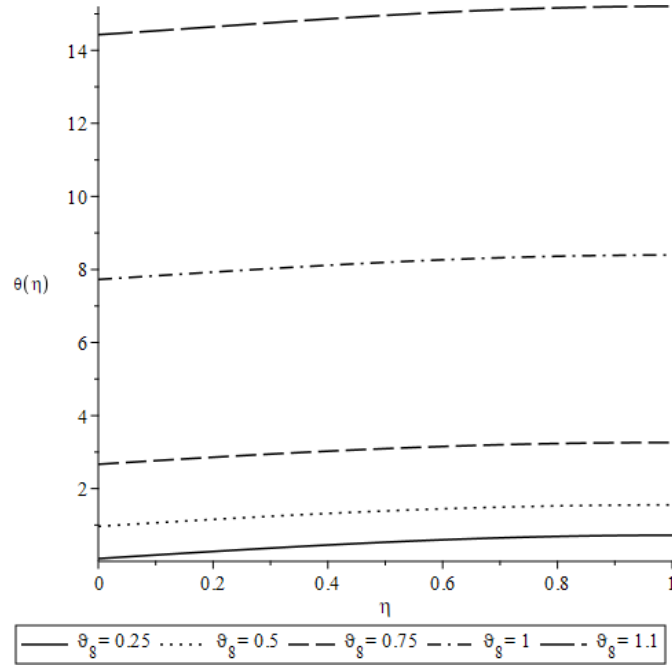


Figure 4. 18: Variation of $\theta(\eta)$ with ϑ_8 ($S = 2.7, \vartheta_4 = \vartheta_5 = \vartheta_7 = \vartheta_{10} = 1, \vartheta_9 = 2.5, Pr = 1$)

2

As P_8 rises, the temperature profile $\theta(\eta)$ moves upward, which is evident from above figure. This means the temperature is increasing. Initially while increasing the value of P_8 , there is a smaller increase in the temperature $\theta(\eta)$. But on further increase in P_8 , the temperature increases significantly as seen in Figure 4.18. The temperature increases significantly between P_8 value of 1.0 and 1.1.

The influence of P_8 on the $\theta(\eta)$ is further explained in the Table 4.5. The table exhibits the influence of P_9 value on the β , $\theta(1)$ and $\theta(0)$. It can be seen that the P_8 plays a significant role in determining the temperature profile. The dimensionless film thickness β remains constant on different values of P_8 value, which is evident from the Table 4.2 as well. So β is independent of P_8 .

Table 4.5: Variation of dimensionless film thickness and free surface temperature with respect to ϑ_8

P_8	β	ϵ	$\theta(1)$
0.3	0.4219431846	0.2292762622	0.8471157752
0.4	0.4219431846	0.5588901223	1.154491095
0.5	0.4219431846	0.9654201059	1.552436625
0.6	0.4219431846	1.491164719	2.077096118
0.7	0.4219431846	2.204094814	2.794947244
0.8	0.4219431846	3.230412584	3.833034864
0.9	0.4219431846	4.838983796	5.463944410
1.0	0.4219431846	7.726055541	8.394826317

1.1	0.4219431846	14.42884897	15.20373682
1.2	0.4219431846	47.29477627	48.59958854

The above table indicates that the free surface temperature $\theta(1)$ and ε are increasing as P_8 increases. This is in agreement with Figure 4.18 i.e. the temperature profile moves upward with increasing value of control parameter P_8 .

The Figure 4.18 and Table 4.5 are given for unsteadiness parameter value equal to 2.7. It is evident from the Table 4.5 and Figure 4.18 that there is a significant increase in the temperature values as P_8 increases beyond 1.0. On the further increase in P_8 value, the distance between temperature profiles becomes wider showing significant increase in temperature value.

The control parameter P_8 value has only a small range in which it can provide optimum temperature profile. It is a very important parameter as seen from the table that a little change of P_8 value from 1.0 onwards has a tremendous influence on the temperature value.

In this chapter, all the factors that control the heat transfer process taking place through a time dependent stretching surface along with variable heat source or sink are studied in detail and the influence of each of the parameters is measured through Maple codes. First HPM is applied and then the influence of each parameter is calculated through iterative procedure on Maple. All the Maple coding is done on the 10th order. So, it gives a very precise and accurate results.

Chapter 5: Conclusion

In this research, the heat transfer process taking place through an extending surface is studied. The complex problem is analyzed using Lie point symmetry analysis technique. A reduction procedure is developed to obtain equations in reduced forms. Lie point symmetry method generates a set of symmetries. Then these symmetries are combined to construct invariants and similarity transformations. As a result, a system of PDEs is reduced to a nonlinear system of ODEs, which is a model consisting of several control parameters.

The system of ODEs is then solved using an analytical solution technique known as Homotopy perturbation method. Multiple solutions are obtained by varying the control parameters one by one. Our system depends on different parameters which include unsteadiness parameter S , Prandtl number Pr , and six additional control parameters i.e.

P_4, P_5, P_7, P_8, P_9 and P_{10} . The influence of each of these parameters on the velocity profile $f'(\eta)$ and temperature profile $\theta(\eta)$ is calculated. Our findings indicate that:

- The most important parameters in this research are the unsteadiness parameter S and the control parameter P_9 value.
- Velocity profile is affected by the unsteadiness parameter S and control variable P_7 . Velocity profile remains unaffected by all the remaining parameters. Velocity profile moves away from the origin with the increase in unsteadiness parameter ' S ' while it moves towards the origin with the increase in the value of control variable P_7 .
- The temperature profile is dependent on S , Pr , and control parameters P_7, P_8 and P_9 . The temperature decreases with the rise in each of S , Pr and control variable P_9 value. While $\theta(\eta)$ rises with the increase in control parameter P_7 and P_8 values.
- The remaining three parameters P_4, P_5 and P_{10} does not affect the temperature and velocity profiles.
- The dimensionless film thickness β is also dependent on the value of S and control parameter P_7 . The β increases with rise in the unsteadiness parameter. While the β decreases with the increase in the control parameter P_7 . The dimensionless film thickness β remains unaffected by remaining parameters i.e. Pr, P_4, P_5, P_8, P_9 , and P_{10} .

Lie point similarity is an important technique that helps to solve complex partial differential equations. It helps to reduce the PDEs to non-linear ordinary differential equations ODE, which is easily solvable. The resulting ODE can be solved by HPM, which is an efficient technique to find analytical solutions and it gives precise and accurate results at a very fast rate. The HPM computational rate of giving result is also very efficient. The research is carried out on the 10th order which gives consistent result as that of 20th order.

In this study, two-dimensional flow is studied. The study can be extended to 3-dimensional flow caused by the extending of the surface in the two lateral directions. The Lie symmetry analysis can be used to reduce the 3-dimensional Navier-Stokes equations into a system of non-linear ordinary differential equations that can be solved using approximate numerical or analytical techniques.

There are a number of analytical solution techniques which can be used to solve the non-linear ordinary differential equations which are obtained through lie point similarity technique. HAM, RKF, FDM, etc. are the names of other analytical solution techniques. The results of HPM can be compared with other methods as well.

These findings are of great importance for the problem of the heat transfer process taking place through an extending surface with variable heat source or sink. The research is helpful in providing novel study of analytical solutions techniques. The methodology and solution technique can further find its role in the flow analysis in different industrial manufacturing processes, and it provides optimum solutions.

References

- 1) Tsai, R., Huang, K.H. and Huang, J.S. (2008) Flow and heat transfer over an unsteady stretching surface with non-uniform heat source, *International Communications in Heat and Mass Transfer*, 35(10), pp. 1340–1343.
- 2) Pal, D. (2011) Combined effects of non-uniform heat source/sink and thermal radiation on heat transfer over an unsteady stretching permeable surface, *Communications in Nonlinear Science and Numerical Simulation*, 16(4), pp. 1890–1904.
- 3) Abel, M.S., Tawade, J. and Nandeppanavar, M.M. (2009) Effect of non-uniform heat source on MHD heat transfer in a liquid film over an unsteady stretching sheet, *International Journal of Non-Linear Mechanics*, 44(9), pp. 990–998.
- 4) Ajaykumar, M., Ajay, C.K. and Srinivasa, A.H. (2023) Effects of viscous dissipation, internal heat source/sink and Prandtl number on flow and heat transfer in a moving fluid over a moving flat surface with an applied magnetic field, *Materials Today: Proceedings*
- 5) Naseer, A.A. et al. (2023) Analytical Solutions for unsteady thin film flow with internal heating and radiation, *Journal of Mathematics*, 2023, pp. 1–12.
- 6) B. C. Sakiadis, Boundary-layer behavior on continuous solid surfaces, *A.I.Ch.E. Journal*, pp. 221-225, 1961.
- 7) Laminar Incompressible Forced Convection-Scientific Figure on ResearchGate. Available from: https://www.researchgate.net/Figure/fig-P55-Control-volume-analysis-of-drag-force-on-a-flat-plate-due-to-boundary-shear_fig20_318040076
- 8) Wen, D. (2013) Nanoparticle-related heat transfer phenomenon and its application in biomedical fields, *Heat Transfer Engineering*, 34(14), pp. 1171–1179.
- 9) Karvinen, R., Rantala, M. and Pesonen, T. (2023) Heat transfer in glass tempering and forming processes, *Proceeding of Advances in Heat Transfer Engineering*, pp. 217–224.
- 10) Lubimova, E.A., Von Herzen, R.P. and Udintsev, G.B. (2013) On heat transfer through the ocean floor, *Geophysical Monograph Series*, pp. 78–86.
- 11) Kido, K. et al. (1996) Temperature dynamic models of heat exchanger for photosensitive material coating and drying processes, *Heat Transfer - Japanese Research*, 25(3), pp. 151–165.
- 12) Wang, C., Liquid film on an unsteady stretching surface. *Quarterly of applied Mathematics*, 1990. 48(4): p. 601-610.
- 13) Andersson, H.I., J.B. Aarseth, and B.S. Dandapat, Heat transfer in a liquid film on an unsteady stretching surface. *International Journal of Heat and Mass Transfer*, 2000. 43(1): p. 69-74.
- 14) Wang, C., Analytic solutions for a liquid film on an unsteady stretching surface. *Heat and Mass Transfer*, 2006. 42(8): p. 759-766.

- 15) Liu, I.C. and H.I. Andersson, Heat transfer in a liquid film on an unsteady stretching sheet. *International Journal of Thermal Sciences*, 2008. 47(6): p. 766-772.
- 16) Dandapat, B., B. Santra, and K. Vajravelu, The effects of variable fluid properties and thermocapillarity on the flow of a thin film on an unsteady stretching sheet. *International Journal of Heat and Mass Transfer*, 2007. 50(5-6): p. 991-996.
- 17) Aziz, R.C. and I. Hashim, Liquid film on unsteady stretching sheet with general surface temperature and viscous dissipation. *Chinese Physics Letters*, 2010. 27(11): p. 110202.
- 18) Noor, N. and I. Hashim, Thermocapillarity and magnetic field effects in a thin liquid film on an unsteady stretching surface. *International Journal of Heat and Mass Transfer*, 2010. 53(9-10): p. 2044-2051.
- 19) Aziz, R.C., I. Hashim, and A. Alomari, Thin film flow and heat transfer on an unsteady stretching sheet with internal heating. *Meccanica*, 2011. 46(2): p. 349-357.
- 20) Salleh, M., Nazar, R., & Pop, I. (2010). Boundary layer flow and heat transfer over a stretching sheet with Newtonian heating. *Journal of the Taiwan Institute of Chemical Engineers*, 41(6), 651–655.
- 21) Megahed, A.M., HPM for the slip velocity effect on a liquid film over an unsteady stretching surface with variable heat flux. *The European Physical Journal Plus*, 2011. 126(9): p. 1-8.
- 22) Liu, I. and A. Megahed, Numerical study for the flow and heat transfer in a thin liquid film over an unsteady stretching sheet with variable fluid properties in the presence of thermal radiation. *Journal of Mechanics*, 2012. 28(2): p. 291-297.
- 23) Liu, I. and A.M. Megahed, Homotopy perturbation method for thin film flow and heat transfer over an unsteady stretching sheet with internal heating and variable heat flux. *Journal of Applied Mathematics*, 2012. 2012.
- 24) Mahmoud, M.A. and A.M. Megahed, MHD flow and heat transfer in a non-Newtonian liquid film over an unsteady stretching sheet with variable fluid properties. *Canadian Journal of Physics*, 2009. 87(10): p. 1065-1071.
- 25) Idrees, M., et al., A similarity solution of time dependent MHD liquid film flow over stretching sheet with variable physical properties. *Results in physics*, 2018. 8: p. 194- 205.
- 26) Rehman, A., Z. Salleh, and T. Gul, Heat transfer of thin film flow over an unsteady stretching sheet with dynamic viscosity. *Journal of Advanced Research in Fluid Mechanics and Thermal Sciences*, 2021. 81(2): p. 67-81
- 27) Elsayed M.A. Elbasha, Dalia A. Aldawody, Heat transfer over an unsteady stretching surface with variable heat flux in the presence of a heat source or sink. *Journal of Computers and Mathematics with Applications*, (2010) p. 2806-2811
- 28) L. J. Crane, Flow past a stretching plate, *Journal of Applied Mathematics and Physics* pp. 645-647, 1970.

- 29) J. Vlegaar, Laminar boundary-layer behaviour on continuous, accelerating surfaces, *Chemical Engineering Science*, vol. 32, no. 12, pp. 1517-1525, 1977.
- 30) P. S. Gupta and A. S. Gupta, Heat and mass transfer on a stretching sheet with suction or blowing, *The Canadian Journal of Chemical Engineering*, pp. 744-746, 1977.
- 31) P. Carragher and L. J. Crane, Heat Transfer on a continuous stretching sheet, *Journal of Applied Mathematics and Mechanics*, vol. 62, pp. 564-565, 1982.
- 32) D. R. Jeng, T. C. A. Chang, and K. J. De Witt, Momentum and heat transfer on a continuous moving surface, *Journal of Heat Transfer*, vol. 108, no. 32, 1986.
- 33) M. Kumari, H. S. Takhar, and G. Nath, MHD flow and heat transfer over a stretching surface with prescribed wall temperature or heat flux, *Heat and mass transfer* vol. 25, pp. 331-336, 1990.
- 34) L. J. Grubka and K. M. Bobba, Heat transfer characteristics of a continuous, stretching surface with variable temperature, *ASME J. Heat Transfer*, vol. 107, pp. 248-250, 1985.
- 35) B. K. Dutta, P. Roy, and A. Gupta, Temperature field in flow over a stretching sheet with uniform heat flux, *International Communications in Heat and Mass Transfer*, pp. 89-94, 1985.

Appendix

This section contains the MAPLE codes that are written specifically for this study. The MAPLE codes used for generating similarity transformations, finding suitable ranges of convergence control parameters, and plotting dimensionless velocity and temperature profiles are given in this section.

> restart:printlevel:=2:with(PDEtools):declare(u(t,x,y),v(t,x,y),T(t,x,y)):

u(t,x,y) will now be displayed as u
v(t,x,y) will now be displayed as v
T(t,x,y) will now be displayed as T

(1)

> sys:={diff(u(t,x,y),x)+diff(v(t,x,y),y)=0,diff(u(t,x,y),t)+u(t,x,y)*diff(u(t,x,y),x)+v(t,x,y)*diff(u(t,x,y),y)=(mu/rho)*diff(u(t,x,y),y,y),diff(T(t,x,y),t)+u(t,x,y)*diff(T(t,x,y),x)+v(t,x,y)*diff(T(t,x,y),y)=(kappa/(rho*C[p]))*diff(T(t,x,y),y,y)+(Q*(T(t,x,y)-a[0])/(rho*C[p])));cond[1]:=y=0;cond[2]:=u-F[1](x,t);cond[3]:=v;cond[4]:=T[y]+F[2](x,t)/kappa;cond[5]:=y-h(t);cond[6]:=v-diff(h(t),t);cond[7]:=u[y];cond[8]:=T[y];

$$\text{sys} := \left\{ u_x + v_y = 0, T_t + u T_x + v T_y = \frac{\kappa T_{y,y}}{\rho C_p} + \frac{Q(T - a_0)}{\rho C_p}, u_t + u u_x + v u_y = \frac{\mu u_{y,y}}{\rho} \right\}$$

cond := table([])

cond₁ := y = 0

cond₂ := u - F₁(x, t)

cond₃ := v

cond₄ := T_y + $\frac{F_2(x, t)}{\kappa}$

cond₅ := y - h(t)

cond₆ := v - h_t

cond₇ := u_y

cond₈ := T_y

(2)

> sym:=Infinitesimals(sys);nops(%);

sym := [-ξ_t(t,x,y,T,u,v)=1, -ξ_x(t,x,y,T,u,v)=0, -ξ_y(t,x,y,T,u,v)=-F₁(t,x), -η_T(t,x,y,T,u,v)=0, -η_u(t,x,y,T,u,v)=0, -η_v(t,x,y,T,u,v)=-F_{1x}u + F_{1t}], [-ξ_t(t,x,y,T,u,v)=0, -ξ_x(t,x,y,T,u,v)=1, -ξ_y(t,x,y,T,u,v)=-F₂(t,x), -η_T(t,x,y,T,u,v)=0, -η_u(t,x,y,T,u,v)=0, -η_v(t,x,y,T,u,v)=-F_{2x}u + F_{2t}], [-ξ_t(t,x,y,T,u,v)=0, -ξ_x(t,x,y,T,u,v)=t, -ξ_y(t,x,y,T,u,v)=-F₃(t,x), -η_T(t,x,y,T,u,v)=0, -η_u(t,x,y,T,u,v)=1, -η_v(t,x,y,T,u,v)=-F_{3x}u + F_{3t}], [-ξ_t(t,x,y,T,u,v)=0, -ξ_x(t,x,y,T,u,v)=x, -ξ_y(t,x,y,T,u,v)=-η_T(t,x,y,T,u,v)=0, -η_u(t,x,y,T,u,v)=u, -η_v(t,x,y,T,u,v)=-F₄(t,x), -ξ_t(t,x,y,T,u,v)=0, -ξ_x(t,x,y,T,u,v)=0, -ξ_y(t,x,y,T,u,v)=-F_{4x}u + F_{4t}], [-ξ_t(t,x,y,T,u,v)=0, -ξ_x(t,x,y,T,u,v)=0, -ξ_y(t,x,y,T,u,v)=-F₅(t,x), -η_T(t,x,y,T,u,v)=T - a₀,

$$\begin{aligned}
& + _F5_t], \left[_ \xi_t(t, x, y, T, u, v) = 0, _ \xi_x(t, x, y, T, u, v) = 0, _ \xi_y(t, x, y, T, u, v) = _F6(t, x), \right. \\
& \left. _ \eta_T(t, x, y, T, u, v) = e^{\frac{Qt}{\rho C_p}}, _ \eta_u(t, x, y, T, u, v) = 0, _ \eta_v(t, x, y, T, u, v) = _F6_x u + _F6_t], \right. \\
& \left[_ \xi_t(t, x, y, T, u, v) = t, _ \xi_x(t, x, y, T, u, v) = 0, _ \xi_y(t, x, y, T, u, v) = \frac{y}{2} + _F7(t, x), _ \eta_T(t, x, \right. \\
& \left. y, T, u, v) = \frac{(T - a_0) Qt}{\rho C_p}, _ \eta_u(t, x, y, T, u, v) = -u, _ \eta_v(t, x, y, T, u, v) = -\frac{v}{2} + _F7_x u \right. \\
& \left. + _F7_t \right]
\end{aligned}$$

Error, invalid input: nops expects 1 argument, but received 7

```
> _F1(t, x) := 0: _F2(t, x) := 0: _F3(t, x) := 0: _F4(t, x) := 0: _F5(t, x) :=
0: _F6(t, x) := 0: _F7(t, x) := 0: _F8(t, x) := 0: _F9(t, x) := 0: _F10(t, x)
:= 0: _F11(t, x) := 0:
```

```
> for i from 1 to 7 do symm[i] := sym[i] end do: #loop on no of
symmetries
```

```
> for j from 1 to 7 do #loop on no of symmetries
for i from 1 to 6 do #loop on no of independent and dependent
variables
```

```
xi[i, j] := rhs(symm[j][i])
```

```
end do
```

```
end do:
```

```
> DepVars := ([T(t, x, y), u(t, x, y), v(t, x, y)]);
DepVars := [T, u, v]
```

(3)

```
> for k from 1 to 7 do S[k] := [lambda[k]*xi[1, k], lambda[k]*xi[2, k],
lambda[k]*xi[3, k], lambda[k]*xi[4, k], lambda[k]*xi[5, k], lambda[k]*
xi[6, k]] end do: for m from 1 to 7 do G[m] := InfinitesimalGenerator
(S[m], DepVars, prolongation = 1, expanded) end do: #loop on no of
symmetries
```

```
> S[1]+S[2]+S[3]+S[4]+S[5]+S[6]+S[7]:G:=InfinitesimalGenerator(%,
DepVars, prolongation = 1, expanded);
```

$$G := f \rightarrow (t\lambda_7 + \lambda_1) \left(\frac{\partial}{\partial t} f \right) + (t\lambda_3 + x\lambda_4 + \lambda_2) \left(\frac{\partial}{\partial x} f \right) + \frac{1}{2} \lambda_7 y \left(\frac{\partial}{\partial y} f \right) \quad (4)$$

$$+ \left(\frac{\lambda_7 (T - a_0) Qt}{\rho C_p} + \lambda_6 e^{\frac{Qt}{\rho C_p}} + \lambda_5 (T - a_0) \right) \left(\frac{\partial}{\partial T} f \right) + (u\lambda_4 - u\lambda_7 + \lambda_3) \left(\frac{\partial}{\partial u} f \right)$$

$$- \frac{1}{2} \lambda_7 v \left(\frac{\partial}{\partial v} f \right)$$

$$\begin{aligned}
& + \frac{1}{\rho C_p} \left[\left(T_t \lambda_7 Q t + \rho C_p T_t \lambda_5 - \lambda_7 T_t \rho C_p - \lambda_3 T_x \rho C_p + \lambda_6 Q e^{\frac{Q t}{\rho C}} + \lambda_7 Q T \right. \right. \\
& \left. \left. - \lambda_7 Q a_0 \right) \left(\frac{\partial}{\partial T_t} f \right) \right] + (-\lambda_3 u_x + \lambda_4 u_t - 2 \lambda_7 u_t) \left(\frac{\partial}{\partial u_t} f \right) + \left(-\frac{3}{2} v_t \lambda_7 \right. \\
& \left. - \lambda_3 v_x \right) \left(\frac{\partial}{\partial v_t} f \right) + \frac{T_x (Q t \lambda_7 - \rho C_p \lambda_4 + \rho C_p \lambda_5)}{\rho C_p} \left(\frac{\partial}{\partial T_x} f \right) - u_x \lambda_7 \left(\frac{\partial}{\partial u_x} f \right) + \left(\right. \\
& \left. -\frac{1}{2} v_x \lambda_7 - \lambda_4 v_x \right) \left(\frac{\partial}{\partial v_x} f \right) + \frac{1}{2} \frac{T_y (2 Q t \lambda_7 + 2 \rho C_p \lambda_5 - \rho C_p \lambda_7)}{\rho C_p} \left(\frac{\partial}{\partial T_y} f \right) + \left(u_y \lambda_4 \right. \\
& \left. - \frac{3}{2} u_y \lambda_7 \right) \left(\frac{\partial}{\partial u_y} f \right) - v_y \lambda_7 \left(\frac{\partial}{\partial v_y} f \right)
\end{aligned}$$

```

> for l from 1 to 8 do #loop on no of conditions
eq[l] := G(cond[l])
end do;

```

```
l := 1
```

```
eq := table([ ])
```

$$eq_1 := \frac{\lambda_7 y}{2} = 0$$

```
l := 2
```

$$eq_2 := -(\lambda_7 t + \lambda_1) (F_1)_t - (\lambda_3 t + \lambda_4 x + \lambda_2) (F_1)_x + \lambda_4 u - \lambda_7 u + \lambda_3$$

```
l := 3
```

$$eq_3 := -\frac{\lambda_7 v}{2}$$

```
l := 4
```

$$eq_4 := \frac{(\lambda_7 t + \lambda_1) (F_2)_t}{\kappa} + \frac{(\lambda_3 t + \lambda_4 x + \lambda_2) (F_2)_x}{\kappa} + \frac{T_y (2 \lambda_7 Q t + 2 \lambda_5 \rho C_p - \lambda_7 \rho C_p)}{2 \rho C_p}$$

```
l := 5
```

$$eq_5 := -(\lambda_7 t + \lambda_1) h_t + \frac{\lambda_7 y}{2}$$

```
l := 6
```

$$eq_6 := -(\lambda_7 t + \lambda_1) h_{t,t} - \frac{\lambda_7 v}{2}$$

```
l := 7
```

$$eq_7 := u_y \lambda_4 - \frac{3}{2} u_y \lambda_7$$

$$l := 8$$

$$eq_8 := \frac{T_y (2 \lambda_7 Q t + 2 \lambda_5 \rho C_p - \lambda_7 \rho C_p)}{2 \rho C_p}$$

$$l := 9 \quad (5)$$

> subs(u=F[1](x,t), eq[2]): pdsolve(%); subs(T[y]=-F[2](x,t)/kappa, eq[4]): pdsolve(%); subs(y=h(t), eq[5]): dsolve(%); eq[1]; eq[3]; eq[6]; eq[7]; eq[8];

$$F_1(x, t) = -\frac{\lambda_3}{\lambda_4 - \lambda_7} + (\lambda_7 t + \lambda_1)^{\frac{\lambda_4}{\lambda_7}}$$

$$-1 \left[\frac{(t \lambda_3 \lambda_4 + x \lambda_4^2 - \lambda_4 \lambda_7 x + \lambda_1 \lambda_3 + \lambda_2 \lambda_4 - \lambda_2 \lambda_7) (\lambda_7 t + \lambda_1)^{-\frac{\lambda_4}{\lambda_7}}}{\lambda_4 (\lambda_4 - \lambda_7)} \right]$$

$$F_2(x, t) = -1 \left[\frac{(t \lambda_3 \lambda_4 + x \lambda_4^2 - \lambda_4 \lambda_7 x + \lambda_1 \lambda_3 + \lambda_2 \lambda_4 - \lambda_2 \lambda_7) (\lambda_7 t + \lambda_1)^{-\frac{\lambda_4}{\lambda_7}}}{\lambda_4 (\lambda_4 - \lambda_7)} \right] (\lambda_7 t$$

$$+ \lambda_1)^{\frac{\lambda_5}{\lambda_7} - \frac{1}{2} - \frac{Q \lambda_1}{\rho C_p \lambda_7} - \frac{Q t}{\rho C_p}}$$

$$h(t) = -CI \sqrt{\lambda_7 t + \lambda_1}$$

$$\frac{\lambda_7 y}{2} = 0$$

$$-\frac{\lambda_7 v}{2}$$

$$-(\lambda_7 t + \lambda_1) h_{t,t} - \frac{\lambda_7 v}{2}$$

$$u_y \lambda_4 - \frac{3}{2} u_y \lambda_7$$

$$\frac{T_y (2 \lambda_7 Q t + 2 \lambda_5 \rho C_p - \lambda_7 \rho C_p)}{2 \rho C_p} \quad (6)$$

> inv[1] := J(t, x, y, T, u, v) : G(inv[1]) : pdsolve(%);

(7)

$$J(t, x, y, T, u, v) = {}_F12 \left[\frac{(t\lambda_3\lambda_4 + x\lambda_4^2 - \lambda_4\lambda_7x + \lambda_1\lambda_3 + \lambda_2\lambda_4 - \lambda_2\lambda_7)(\lambda_7t + \lambda_1)^{-\frac{\lambda_4}{\lambda_7}}}{\lambda_4(\lambda_4 - \lambda_7)}, \right. \\ \left. \frac{y}{\sqrt{\lambda_7t + \lambda_1}}, \frac{1}{-\lambda_5\rho C_p + Q\lambda_1} \left((\lambda_7t + \lambda_1)^{\frac{-\lambda_5\rho C_p + Q\lambda_1}{\lambda_7\rho C_p}} \left(-\lambda_5 T \rho C_p e^{-\frac{Q}{\rho C_p}t} \right. \right. \right. \\ \left. \left. \left. + e^{-\frac{Q}{\rho C_p}t} \rho C_p a_0 \lambda_5 + T Q \lambda_1 e^{-\frac{Q}{\rho C_p}t} - Q a_0 \lambda_1 e^{-\frac{Q}{\rho C_p}t} - \rho C_p \lambda_6 \right) \right), \frac{\lambda_4}{-\lambda_7} \right. \\ \left. \frac{(ut\lambda_4\lambda_7 - ut\lambda_7^2 + t\lambda_3\lambda_7 \quad \lambda_4\lambda_4 + \lambda_7 \quad \lambda_1\lambda_7 + \lambda_1\lambda_3)(\lambda_7t + \lambda_1)^{-u}}{\lambda_4(\lambda_4 - \lambda_7)}, v \sqrt{\lambda_7t + \lambda_1} \right] \quad (7)$$

> **#Step Four (write system in new variables and find its symmetries) :**

> #Step Four (write system in new variables and find its symmetries):

```
> declare(for i from 1 to 3 do F[i]((t*lambda[3]*lambda
[4] + x*lambda[4]^2 - x*lambda[4]*lambda[7] + lambda[1]
*lambda[3] + lambda[2]*lambda[4] - lambda[2]*lambda[7])
*(t*lambda[7] + lambda[1])^(-lambda[4]/lambda[7]) /
(lambda[4]*(lambda[4] - lambda[7])), y/sqrt(t*lambda[7]
+ lambda[1])) end do):
```

$$F \left[\frac{(t\lambda_3\lambda_4 + x\lambda_4^2 - \lambda_4\lambda_7x + \lambda_1\lambda_3 + \lambda_2\lambda_4 - \lambda_2\lambda_7)(\lambda_7t + \lambda_1)^{-\frac{\lambda_4}{\lambda_7}}}{\lambda_4(\lambda_4 - \lambda_7)}, \right. \\ \left. \frac{y}{\sqrt{\lambda_7t + \lambda_1}}, \frac{1}{-\lambda_5\rho C_p + Q\lambda_1} \left((\lambda_7t + \lambda_1)^{\frac{-\lambda_5\rho C_p + Q\lambda_1}{\lambda_7\rho C_p}} \left(-\lambda_5 T \rho C_p e^{-\frac{Q}{\rho C_p}t} \right. \right. \right. \\ \left. \left. \left. + e^{-\frac{Q}{\rho C_p}t} \rho C_p a_0 \lambda_5 + T Q \lambda_1 e^{-\frac{Q}{\rho C_p}t} - Q a_0 \lambda_1 e^{-\frac{Q}{\rho C_p}t} - \rho C_p \lambda_6 \right) \right), \frac{\lambda_4}{-\lambda_7} \right. \\ \left. \frac{(ut\lambda_4\lambda_7 - ut\lambda_7^2 + t\lambda_3\lambda_7 \quad \lambda_4\lambda_4 + \lambda_7 \quad \lambda_1\lambda_7 + \lambda_1\lambda_3)(\lambda_7t + \lambda_1)^{-u}}{\lambda_4(\lambda_4 - \lambda_7)}, v \sqrt{\lambda_7t + \lambda_1} \right] \quad (8)$$

$$\left. \frac{y}{\sqrt{\lambda_7 t + \lambda_1}} \right\} \text{will now be displayed as } F$$

```
> var1:=simplify(solve((t*u*lambda[4]*lambda[7] - t*u*
lambda[7]^2 + t*lambda[3]*lambda[7] + u*lambda[1]*
lambda[4] - u*lambda[1]*lambda[7] + lambda[1]*lambda[3]
)* (t*lambda[7] + lambda[1])^(-lambda[4]/lambda[7])/
(lambda[4] - lambda[7])= F[1], u)):
```

```
> var2:=simplify(solve(v*sqrt(t*lambda[7] + lambda[1])=F
[2], v)):
```

```
> var3:=simplify(solve((t*lambda[7] + lambda[1])^((-rho*C
[p]*lambda[5] + Q*lambda[1])/(rho*C[p]*lambda[7]))*(-
lambda[5]*T*rho*C[p]*exp(-Q*t/(rho*C[p])) + exp(-Q*t/
(rho*C[p]))*C[p]*rho*a[0]*lambda[5] + T*Q*lambda[1]*exp
(-Q*t/(rho*C[p])) - Q*a[0]*lambda[1]*exp(-Q*t/(rho*C[p]
)) - rho*C[p]*lambda[6])/(-rho*C[p]*lambda[5] + Q*
lambda[1])=F[3], T)):
```

```
> u:=(F[1]((t*lambda[3]*lambda[4] + x*lambda[4]^2 - x*
lambda[4]*lambda[7] + lambda[1]*lambda[3] + lambda[2]*
lambda[4] - lambda[2]*lambda[7])*(t*lambda[7] + lambda
[1])^(-lambda[4]/lambda[7])/(lambda[4]*(lambda[4] -
lambda[7])), y/sqrt(t*lambda[7] + lambda[1]))*(lambda
[4] - lambda[7])*(t*lambda[7] + lambda[1])^(lambda[4]
/lambda[7] - lambda[3]*(t*lambda[7] + lambda[1]))/(
(lambda[4] - lambda[7])*(t*lambda[7] + lambda[1])));
```

$$u := \frac{F_1(\lambda_4 - \lambda_7) (\lambda_7 t + \lambda_1)^{\frac{\lambda_4}{\lambda_7}} - \lambda_3 (\lambda_7 t + \lambda_1)}{(\lambda_4 - \lambda_7) (\lambda_7 t + \lambda_1)}$$

(9)

```
> v:=F[2]((t*lambda[3]*lambda[4] + x*lambda[4]^2 - x*
lambda[4]*lambda[7] + lambda[1]*lambda[3] + lambda[2]*
lambda[4] - lambda[2]*lambda[7])*(t*lambda[7] + lambda
[1])^(-lambda[4]/lambda[7])/(lambda[4]*(lambda[4] -
lambda[7])), y/sqrt(t*lambda[7] + lambda[1]))/sqrt(t*
```

lambda[7] + lambda[1]);

$$v := \frac{F_2}{\sqrt{\lambda_7 t + \lambda_1}} \quad (10)$$

> T := (exp(Q*t/(rho*C[p]))*F[3]((t*lambda[3]*lambda[4] + x*lambda[4]^2 - x*lambda[4]*lambda[7] + lambda[1]*lambda[3] + lambda[2]*lambda[4] - lambda[2]*lambda[7]))*(t*lambda[7] + lambda[1])^(-lambda[4]/lambda[7]))/(lambda[4]*(lambda[4] - lambda[7])), y/sqrt(t*lambda[7] + lambda[1]))*(-rho*C[p]*lambda[5] + Q*lambda[1])*(t*lambda[7] + lambda[1])^((rho*C[p]*lambda[5] - Q*lambda[1])/(rho*C[p]*lambda[7])) + rho*C[p]*lambda[6]*exp(Q*t/(rho*C[p])) + a[0]*(-rho*C[p]*lambda[5] + Q*lambda[1]))/(-rho*C[p]*lambda[5] + Q*lambda[1]);

T := (11)

$$\frac{1}{-\lambda_5 \rho C_p + Q \lambda_1} \left(e^{\frac{Q t}{\rho C_p}} F_3 \left(-\lambda_5 \rho C_p + Q \lambda_1 \right) \left(\lambda_7 t + \lambda_1 \right)^{\frac{\lambda_5 \rho C_p - Q \lambda_1}{\lambda_7 \rho C_p}} + \lambda_6 e^{\frac{Q t}{\rho C_p}} \rho C_p + a_0 \left(-\lambda_5 \rho C_p + Q \lambda_1 \right) \right)$$

> eq1 := diff(u, x) + diff(v, y) = 0 : simplify(%):

> eq2 := diff(u, t) + u*diff(u, x) + v*diff(u, y) - (mu/rho)*diff(u, y, y) = 0 : simplify(%):

> eq3 := diff(T, t) + u*diff(T, x) + v*diff(T, y) - ((kappa/(rho*C[p]))) * diff(T, y, y) - (Q*(T-a[0])/(rho*C[p])) = 0 : simplify(%):

> conds1 := diff(u, y) : conds2 := diff(T, y) :

conds2 := (12)

$$\frac{1}{\sqrt{\lambda_7 t + \lambda_1}} \left(e^{\frac{Q t}{\rho C_p}} D_2(F_3) \left(\frac{1}{\lambda_4 (\lambda_4 - \lambda_7)} \left((t \lambda_3 \lambda_4 + x \lambda_4^2 - \lambda_4 \lambda_7 x + \lambda_1 \lambda_3 + \lambda_2 \lambda_4 - \lambda_2 \lambda_7) (\lambda_7 t + \lambda_1)^{-\frac{\lambda_4}{\lambda_7}} \right), \frac{y}{\sqrt{\lambda_7 t + \lambda_1}} \right) \left(\lambda_7 t + \lambda_1 \right)^{\frac{\lambda_5 \rho C_p - Q \lambda_1}{\lambda_7 \rho C_p}} \right)$$

```

> with(MTM):printlevel:=2:
for j from 1 to 2 do
for i from 1 to 3 do
F[i]((t*lambda[3]*lambda[4] + x*lambda[4]^2 - x*lambda
[4]*lambda[7] + lambda[1]*lambda[3] + lambda[2]*lambda
[4] - lambda[2]*lambda[7])*(t*lambda[7] + lambda[1])^(-
lambda[4]/lambda[7])/(lambda[4]*(lambda[4] - lambda[7])
), y/sqrt(t*lambda[7] + lambda[1])):=F[i];
D[j](F[i])((t*lambda[3]*lambda[4] + x*lambda[4]^2 - x*
lambda[4]*lambda[7] + lambda[1]*lambda[3] + lambda[2]*
lambda[4] - lambda[2]*lambda[7])*(t*lambda[7] + lambda
[1])^(-lambda[4]/lambda[7])/(lambda[4]*(lambda[4] -
lambda[7]))), y/sqrt(t*lambda[7] + lambda[1])):=F[i,z[j]
];
D[j,j](F[i])((t*lambda[3]*lambda[4] + x*lambda[4]^2 -
x*lambda[4]*lambda[7] + lambda[1]*lambda[3] + lambda[2]
*lambda[4] - lambda[2]*lambda[7])*(t*lambda[7] + lambda
[1])^(-lambda[4]/lambda[7])/(lambda[4]*(lambda[4] -
lambda[7]))), y/sqrt(t*lambda[7] + lambda[1])):=F[i,z
[j],z[j]];
end do
end do:

```

```

> simplify(eq1);

```

$$\frac{F_{1,z_1} + F_{2,z_2}}{\lambda_7 t + \lambda_1} = 0 \quad (13)$$

```

> simplify(eq2);

```

$$\frac{1}{2\rho(\lambda_4 - \lambda_7)(\lambda_7 t + \lambda_1)^2} \left(-\lambda_7 F_{1,z_2} y \rho(\lambda_4 - \lambda_7)(\lambda_7 t + \lambda_1)^{\frac{2\lambda_4 - \lambda_7}{2\lambda_7}} + 2 \left((F_1 F_{1,z_1} + \lambda_4 F_1 - \lambda_7 F_1 + F_2 F_{1,z_2}) \rho - \mu F_{1,z_2,z_2} \right) (\lambda_4 - \lambda_7)(\lambda_7 t + \lambda_1)^{\frac{\lambda_4}{\lambda_7}} - 2 F_{1,z_1} (x \lambda_4^2 \right) \quad (14)$$

$$\left. + (\lambda_3 t - x \lambda_7 + \lambda_2) \lambda_4 + \lambda_1 \lambda_3 - \lambda_2 \lambda_7 \right) \rho = 0$$

> **simplify(eq3);**

$$-\frac{1}{\rho C_p (\lambda_4 - \lambda_7)} \left[e^{\frac{Q t}{\rho C_p}} \left(\frac{\rho C_p \gamma F_{3,z_2} \lambda_7 (\lambda_4 - \lambda_7) (\lambda_7 t + \lambda_1)}{2} \frac{2\rho \left(\lambda_5 - \frac{3\lambda_7}{2} \right) C_p - 2Q\lambda_1}{2\rho C_p \lambda_7} \right) \right] \quad (15)$$

$$\begin{aligned} & + \rho \left(x \lambda_4^2 + (\lambda_3 t - x \lambda_7 + \lambda_2) \lambda_4 + \lambda_1 \lambda_3 - \lambda_2 \lambda_7 \right) C_p F_{3,z_1} (\lambda_7 t \\ & + \lambda_1) \frac{-\rho(\lambda_4 - \lambda_5 + \lambda_7) C_p - Q\lambda_1}{\rho C_p \lambda_7} + (\lambda_7 t + \lambda_1) \frac{\rho(\lambda_5 - \lambda_7) C_p - Q\lambda_1}{\rho C_p \lambda_7} \left(-\rho \left(F_1 F_{3,z_1} + F_2 F_{3,z_2} \right. \right. \\ & \left. \left. + F_3 \lambda_5 \right) C_p + Q F_3 \lambda_1 + F_{3,z_2,z_2} K \right) (\lambda_4 - \lambda_7) \Bigg) = 0 \end{aligned}$$

> **TT := simplify(expand((eq2)),size):**

if lhs(TT)::`*` and rhs(TT)::`*` then

TTT := map[2](map,freeze,TT);

comm := `*`(op({op(lhs(TTT))} intersect {op(rhs(TTT))}));

new := simplify(thaw(lhs(TTT)/comm=rhs(TTT)/comm));

end if:

new:

> **TT1 := simplify(eq3,size):**

if lhs(TT1)::`*` and rhs(TT1)::`*` then

TTT1 := map[2](map,freeze,TT1);

comm := `*`(op({op(lhs(TTT1))} intersect {op(rhs(TTT1))}));

new := simplify(thaw(lhs(TTT1)/comm=rhs(TTT1)/comm));

end if:

new:simplify(isolate(% ,F[3,z[2],z[2]]):

#(isolate,6): error "%1 does not contain %2", expr, x

Error, (in isolate) new does not contain F[3, z[2], z[2]]

locals defined as: expr1 = expr1, expr2 = expr2, ito = ito, xx = xx, linop = linop, new_args = new_args, subs_args = subs_args, subs_back = subs_back, funcs = funcs

> **restart:with(PDEtools):declare(F[1](z[1],z[2]),F[2](z[1],z[2]),F[3](z[1],z[2]),F[4](z[1],z[2])):**
F(z₁,z₂) will now be displayed as F (16)

> **sys:={diff(F[1](z[1],z[2]),z[1])+diff(F[2](z[1],z[2]),z[2])=0,(lambda[4]-lambda[7])*F[1](z[1],z[2])+(F[1](z[1],z[2])-lambda[4]*z[1])*diff(F[1](z[1],z[2]),z[1])-(lambda[7]*z[2]/2)*diff(F[1](z[1],z[2]),z[2])+F[2](z[1],z[2])*diff(F[1](z[1],z[2]),z[2])-(mu/rho)*diff(F[1](z[1],z[2]),z[2],z[2])=0,(lambda[5]-lambda[1]*Q/(rho*C[p]))*F[3](z[1],z[2])+(F[1](z[1],z[2])-lambda[4]*z[1])*diff(F[3](z[1],z[2]),z[1])-(lambda[7]*z[2]/2)*diff(F[3](z[1],z[2]),z[2])+F[2](z[1],z[2])*diff(F[3](z[1],z[2]),z[2])-(kappa/(rho*C[p]))*diff(F[3](z[1],z[2]),z[2],z[2])=0};**

$$\text{sys} := \left\{ \begin{array}{l} (F_1)_{z_1} + (F_2)_{z_2} = 0, (\lambda_4 - \lambda_7) F_1 + (F_1 - \lambda_4 z_1) (F_1)_{z_1} - \frac{\lambda_7 z_2 (F_1)_{z_2}}{2} + F_2 (F_1)_{z_2} \\ - \frac{\mu (F_1)_{z_2, z_2}}{\rho} = 0, \left(\lambda_5 - \frac{\lambda_1 Q}{\rho C_p} \right) F_3 + (F_1 - \lambda_4 z_1) (F_3)_{z_1} - \frac{\lambda_7 z_2 (F_3)_{z_2}}{2} + F_2 (F_3)_{z_2} \\ - \frac{\kappa (F_3)_{z_2, z_2}}{\rho C_p} = 0 \end{array} \right. \quad (17)$$

> **Infinitesimals(sys);nops(%);**

$$\left[\begin{array}{l} -\xi_{z_1}(z_1, z_2, F_1, F_2, F_3) = 0, -\xi_{z_2}(z_1, z_2, F_1, F_2, F_3) = -F_1(z_1), -\eta_{F_1}(z_1, z_2, F_1, F_2, F_3) = 0, \\ -\eta_{F_2}(z_1, z_2, F_1, F_2, F_3) = -_{F_1 z_1} \lambda_4 z_1 + _{F_1 z_1} F_1 + \frac{-F_1(z_1) \lambda_7}{2}, -\eta_{F_3}(z_1, z_2, F_1, F_2, F_3) \\ = F_3 \end{array} \right], \left[\begin{array}{l} -\xi_{z_1}(z_1, z_2, F_1, F_2, F_3) = z_1, -\xi_{z_2}(z_1, z_2, F_1, F_2, F_3) = -F_2(z_1), -\eta_{F_1}(z_1, z_2, F_1, F_2, F_3) \\ = F_1, -\eta_{F_2}(z_1, z_2, F_1, F_2, F_3) = -_{F_2 z_1} \lambda_4 z_1 + _{F_2 z_1} F_1 + \frac{-F_2(z_1) \lambda_7}{2}, -\eta_{F_3}(z_1, z_2, F_1, F_2, \\ F_3) = 0 \end{array} \right]$$

Error, invalid input: nops expects 1 argument, but received 2

Step Two again :

```
> restart:with(PDEtools,InfinitesimalGenerator,declare,
ToJet,FromJet):
```

```
> DepVars := ([F[1](z[1],z[2]),F[2](z[1],z[2]),F[3](z[1],
z[2])]);
```

$$DepVars := [F_1(z_1, z_2), F_2(z_1, z_2), F_3(z_1, z_2)] \quad (18)$$

```
> S := [lambda[8]*z[1],0,lambda[8]*F[1],0,lambda[9]*F[3]]
;
```

$$S := [\lambda_8 z_1, 0, \lambda_8 F_1, 0, \lambda_9 F_3] \quad (19)$$

```
> G:=InfinitesimalGenerator(S, DepVars, prolongation = 1,
expanded);
```

$$G := f \rightarrow \lambda_8 z_1 \left(\frac{\partial}{\partial z_1} f \right) + \lambda_8 F_1 \left(\frac{\partial}{\partial F_1} f \right) + \lambda_9 F_3 \left(\frac{\partial}{\partial F_3} f \right) - \lambda_8 F_{2z_1} \left(\frac{\partial}{\partial F_{2z_1}} f \right) + \left(-\lambda_8 F_{3z_1} + \lambda_9 F_{3z_1} \right) \left(\frac{\partial}{\partial F_{3z_1}} f \right) + F_{1z_2} \lambda_8 \left(\frac{\partial}{\partial F_{1z_2}} f \right) + F_{3z_2} \lambda_9 \left(\frac{\partial}{\partial F_{3z_2}} f \right) \quad (20)$$

```
> j1:=z[2]=0;j2:=F[1]-f[1](z[1])=0;j3:=F[2]=0;j4:=F[3][z
[2]]+f[2](z[1])/kappa=0;j5:=z[2]-C[1]=0;j6:=F[1][z[2]]=
0;j7:=F[3][z[2]]=0;j8:=F[2]-C[1]/2=0;
```

$$j1 := z_2 = 0$$

$$j2 := F_1 - f_1(z_1) = 0$$

$$j3 := F_2 = 0$$

$$j4 := (F_3)_{z_2} + \frac{f_2(z_1)}{\kappa} = 0$$

$$j5 := z_2 - C_1 = 0$$

$$j6 := (F_1)_{z_2} = 0$$

$$j7 := (F_3)_{z_2} = 0$$

$$j8 := F_2 - \frac{C_1}{2} = 0$$

(21)

```
> eq1:=G(j1);eq2:=G(j2);eq3:=G(j3);eq4:=G(j4);eq5:=G(j5);
eq6:=G(j6);eq7:=G(j7);eq8:=G(j8);
```

$$eq1 := 0 = 0$$

$$eq2 := -\lambda_8 z_1 \left(\frac{d}{dz_1} f_1(z_1) \right) + \lambda_8 F_1 = 0$$

$$\begin{aligned}
eq3 &:= 0=0 \\
eq4 &:= \frac{\lambda_8 z_1 \left(\frac{d}{dz_1} f_2(z_1) \right)}{\kappa} + (F_3)_{z_2} \lambda_9 = 0 \\
eq5 &:= 0=0 \\
eq6 &:= (F_1)_{z_2} \lambda_8 = 0 \\
eq7 &:= (F_3)_{z_2} \lambda_9 = 0 \\
eq8 &:= 0=0
\end{aligned} \tag{22}$$

> subs(F[1]=f[1](z[1]), eq2) : dsolve(%) ; subs(F[3][z[2]]=-f[2](z[1])/kappa, eq4) : dsolve(%) ;

$$\begin{aligned}
f_1(z_1) &= -C_1 z_1 \\
f_2(z_1) &= -C_1 z_1^{\frac{\lambda_9}{\lambda_8}}
\end{aligned} \tag{23}$$

> Step Three again :

> restart:with(PDEtools, InfinitesimalGenerator, declare, ToJet, FromJet) :

> DepVars := ([F[1](z[1], z[2]), F[2](z[1], z[2]), F[3](z[1], z[2])]) ;

$$DepVars := [F_1(z_1, z_2), F_2(z_1, z_2), F_3(z_1, z_2)]$$

> S := [lambda[8]*z[1], 0, lambda[8]*F[1], 0, lambda[9]*F[3]] ;

$$S := [\lambda_8 z_1, 0, \lambda_8 F_1, 0, \lambda_9 F_3]$$

> G:=InfinitesimalGenerator(S, DepVars, prolongation = 1, expanded) ;

$$\begin{aligned}
G := f \rightarrow & \lambda_8 z_1 \left(\frac{\partial}{\partial z_1} f \right) + \lambda_8 F_1 \left(\frac{\partial}{\partial F_1} f \right) + \lambda_9 F_3 \left(\frac{\partial}{\partial F_3} f \right) - \lambda_8 F_{2z_1} \left(\frac{\partial}{\partial F_{2z_1}} f \right) + \left(-\lambda_8 F_{3z_1} \right. \\
& \left. + \lambda_9 F_{3z_1} \right) \left(\frac{\partial}{\partial F_{3z_1}} f \right) + F_{1z_2} \lambda_8 \left(\frac{\partial}{\partial F_{1z_2}} f \right) + F_{3z_2} \lambda_9 \left(\frac{\partial}{\partial F_{3z_2}} f \right)
\end{aligned}$$

> j:=J(z[1], z[2], F[1], F[2], F[3]) : G(j)=0 ; pdsolve(%) ;

$$\begin{aligned}
\lambda_8 z_1 \left(\frac{\partial}{\partial z_1} J(z_1, z_2, F_1, F_2, F_3) \right) + \lambda_8 F_1 \left(\frac{\partial}{\partial F_1} J(z_1, z_2, F_1, F_2, F_3) \right) + \lambda_9 F_3 \left(\frac{\partial}{\partial F_3} J(z_1, z_2, \right. \\
\left. F_1, F_2, F_3) \right) = 0
\end{aligned}$$

$$J(z_1, z_2, F_1, F_2, F_3) = -Fl \left(z_2, \frac{F_1}{z_1}, F_2, F_3 z_1^{-\frac{\lambda_9}{\lambda_8}} \right) \quad (27)$$

> Step Four again :

> `restart:with(PDEtools):declare(P[1](z[2]),P[2](z[2]),P[3](z[2]),P[4](z[2])):`

P(z₂) will now be displayed as P (28)

> `F[1]:=z[1]*P[1](z[2]);F[2]:=P[2](z[2]);F[3]:=(z[1])^(lambda[9]/lambda[8])*P[3](z[2]);`

$$F_1 := z_1 P_1$$

$$F_2 := P_2$$

$$F_3 := z_1^{\frac{\lambda_9}{\lambda_8}} P_3$$

(29)

> `eqred1:=diff(F[1],z[1])+diff(F[2],z[2])=0;eqred2:=(lambda[4]-lambda[7])*F[1]+(F[1]-lambda[4]*z[1])*diff(F[1],z[1])-(lambda[7]*z[2]/2)*diff(F[1],z[2])+F[2]*diff(F[1],z[2])-(mu/rho)*diff(F[1],z[2],z[2])=0;eqred3:=(lambda[5]-lambda[1]*Q/(rho*C[p]))*F[3]+(F[1]-lambda[4]*z[1])*diff(F[3],z[1])-(lambda[7]*z[2]/2)*diff(F[3],z[2])+F[2]*diff(F[3],z[2])-(kappa/(rho*C[p]))*diff(F[3],z[2],z[2])=0;`

$$eqred1 := P_1 + (P_2)_{z_2} = 0$$

$$eqred2 := (\lambda_4 - \lambda_7) z_1 P_1 + (-\lambda_4 z_1 + z_1 P_1) P_1 - \frac{\lambda_7 z_2 z_1 (P_1)_{z_2}}{2} + P_2 z_1 (P_1)_{z_2} - \frac{\mu z_1 (P_1)_{z_2, z_2}}{\rho} = 0$$

$$eqred3 := \left(\lambda_5 - \frac{\lambda_1 Q}{\rho C_p} \right) z_1^{\frac{\lambda_9}{\lambda_8}} P_3 + \frac{(-\lambda_4 z_1 + z_1 P_1) z_1^{\frac{\lambda_9}{\lambda_8}} \lambda_9 P_3}{\lambda_8 z_1} - \frac{\lambda_7 z_2 z_1^{\frac{\lambda_9}{\lambda_8}} (P_3)_{z_2}}{2} + P_2 \quad (30)$$

$$\frac{\lambda_9}{z_1^{\lambda_8}} (P_3)_{z_2} - \frac{\kappa z_1^{\lambda_9} (P_3)_{z_2, z_2}}{\rho C_p} = 0$$

> **diff(F[3], z[2]);**

$$\frac{\lambda_9}{z_1^{\lambda_8}} (P_3)_{z_2}$$

(31)

```
> restart:with(PDEtools):declare(f(x),q(x),prime=x):
      f(x) will now be displayed as f
      q(x) will now be displayed as q
      derivatives with respect to x of functions of one variable will now be displayed with ' (1)
```

```
> N:=10:S:=2.7:Pr:=1:lambda[4]:=1:lambda[5]:=1:lambda[7]:=1:lambda
[8]:=1:lambda[9]:=2.5:lambda[10]:=1:
> m(x):=sum(p^i*f[i](x),i=0..N):n(x):=sum(p^i*q[i](x),i=0..N):
  > eq1:=(1-p)*diff(m(x),x,x,x)+p*(diff(m(x),x,x,x)+r*((lambda[7]/2)
*S*x-m(x))*diff(m(x),x,x)+(diff(m(x),x))^2+S*lambda[7]*diff(m(x),
x))):eq2:=(1-p)*diff(n(x),x,x)+p*(diff(n(x),x,x)+Pr*r*((lambda
[7]*S*x/2)-m(x))*diff(n(x),x)+(lambda[9]/lambda[8])*n(x)*diff(m
(x),x)-S(lambda[5]-lambda[10]-(lambda[4]*lambda[9]/lambda[8]))*n
(x))):
> for i from 0 to N do
  equ[i] := coeff(eq1, p, i) ;
  eqv[i] := coeff(eq2, p, i) ;
end do:
> ics1[0] := f[0](0) = 0, D(f[0])(0) = 1, D(D(f[0]))(0) = alpha:
ics2[0]:=q[0](0)=epsilon,D(q[0])(0) =1:
> dsolve({ics1[0],equ[0]}):f[0](x) := rhs(%);dsolve({ics2[0],eqv[0]
}):q[0](x) := rhs(%) ;
```

$$f_0 \mathbf{d} \frac{1}{2} a x^2 C x$$

$$q_0 \mathbf{d} e C x \quad (2)$$

```
> for i from 1 to N do
  sys1[i]:=- (int(int(int(equ[i],x),x),x))+f[i](x):sys2[i]:=- (int
(int(eqv[i],x),x))+q[i](x):f[i](x):=sys1[i];q[i](x):=sys2[i];
end do:
> f(x):=sum(f[j](x),j=0..N):q(x):=sum(q[j](x),j=0..N):
> eq1 := subs(x = 1, f(x)):
> eq2:=eq1-S/2:
> eq3 := diff(f(x), x, x):
> eq4:=eval(eq3,x=1):sys:={eq2=0, eq4=0}:
> V := fsolve(sys);
```

$$V \mathbf{d} \alpha = 0.9826367844, r = 0.1780360510 \quad (3)$$

```
> eq5:=diff(q(x),x):eq6:=eval(eq5,x=1):eq7:=eval(eq6,V):
> epsilon:=solve(eq7);
```

$$e \mathbf{d} 7.726055541 \quad (4)$$

```
> alpha:=rhs(V[1]);r:=rhs(V[2]);
```

$$a \mathbf{d} 0.9826367844 \quad (5)$$

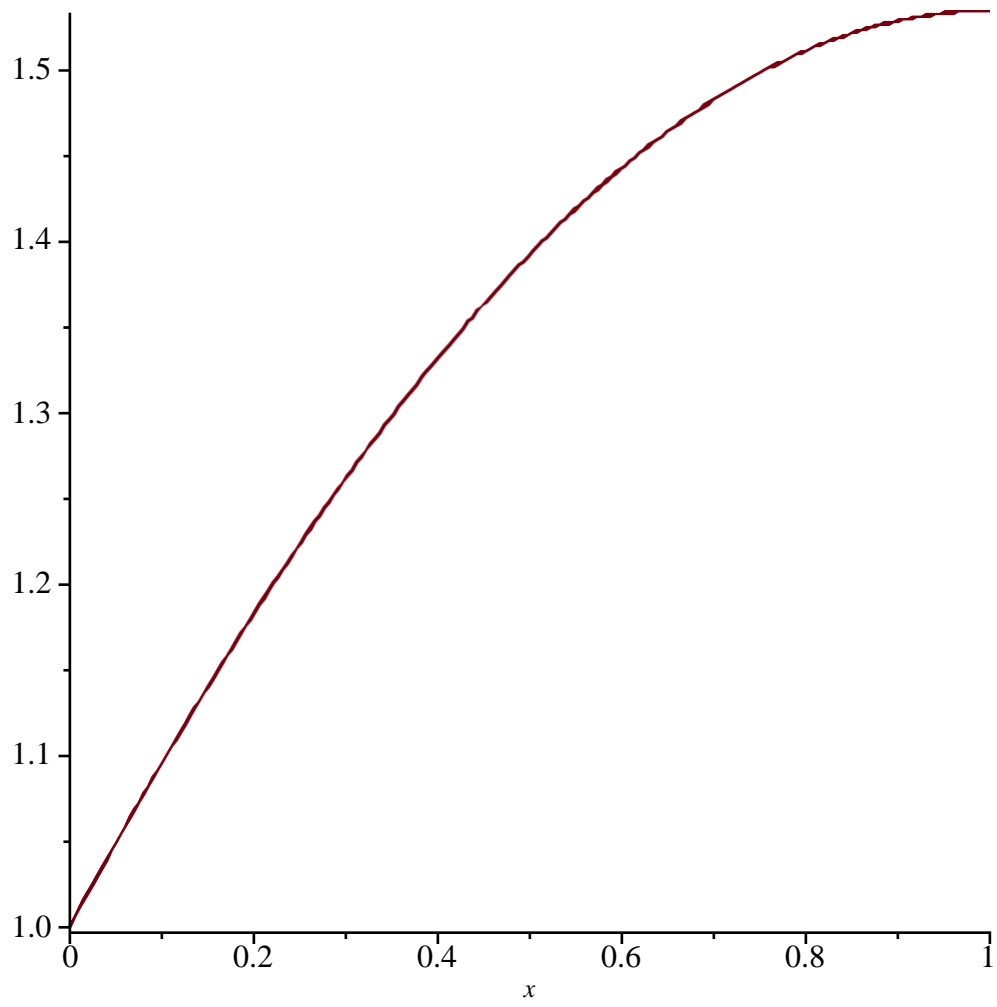
$$r \mathbf{d} 0.1780360510 \quad (5)$$

```
> beta:=sqrt(r);
```

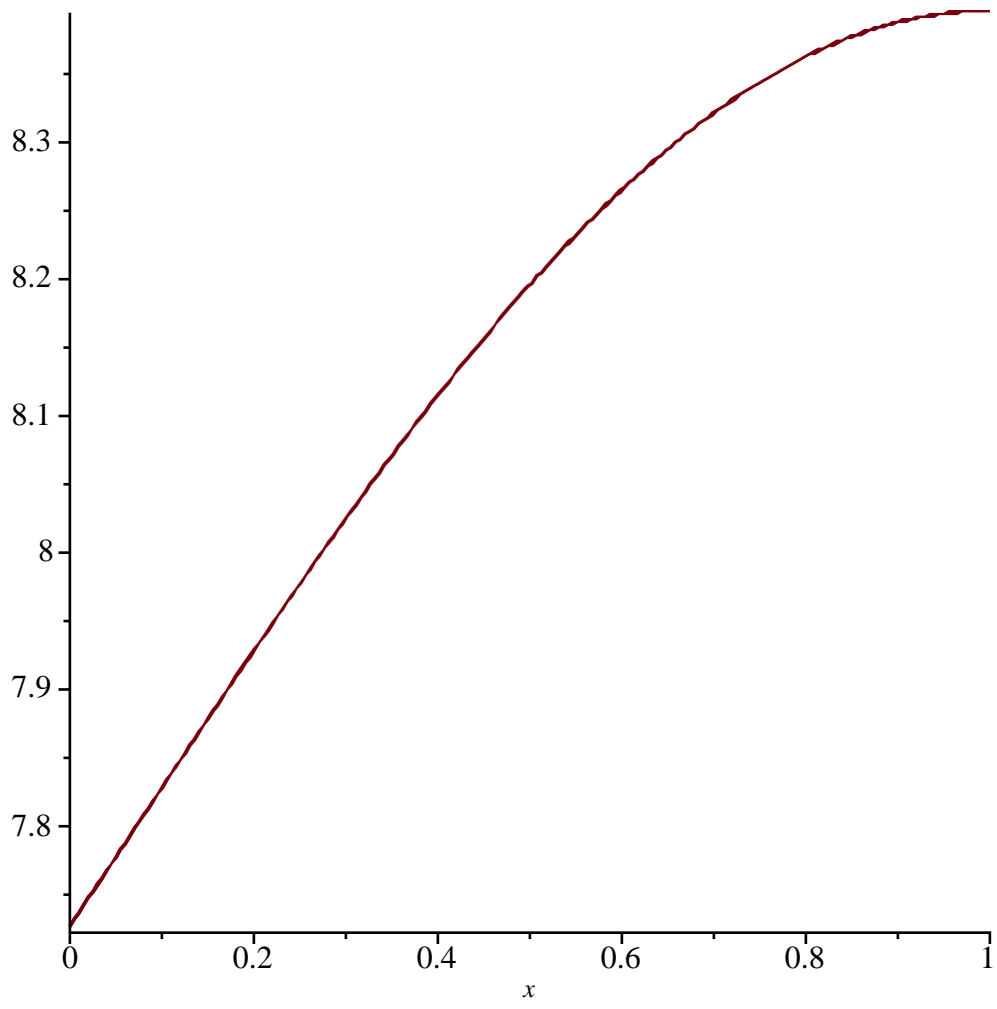
$$b \mathbf{d} 0.4219431846 \quad (6)$$

```
> eq8 := simplify(f(x), size):eq9:=diff(eq8,x):eq10:=simplify(q(x),
size):
```

```
> plot(eq9,x=0..1);
```



```
> plot(eq10,x=0..1);
```



```
> eval(eq10, x=1);
```

8.394826317

(7)